

Figure 1:

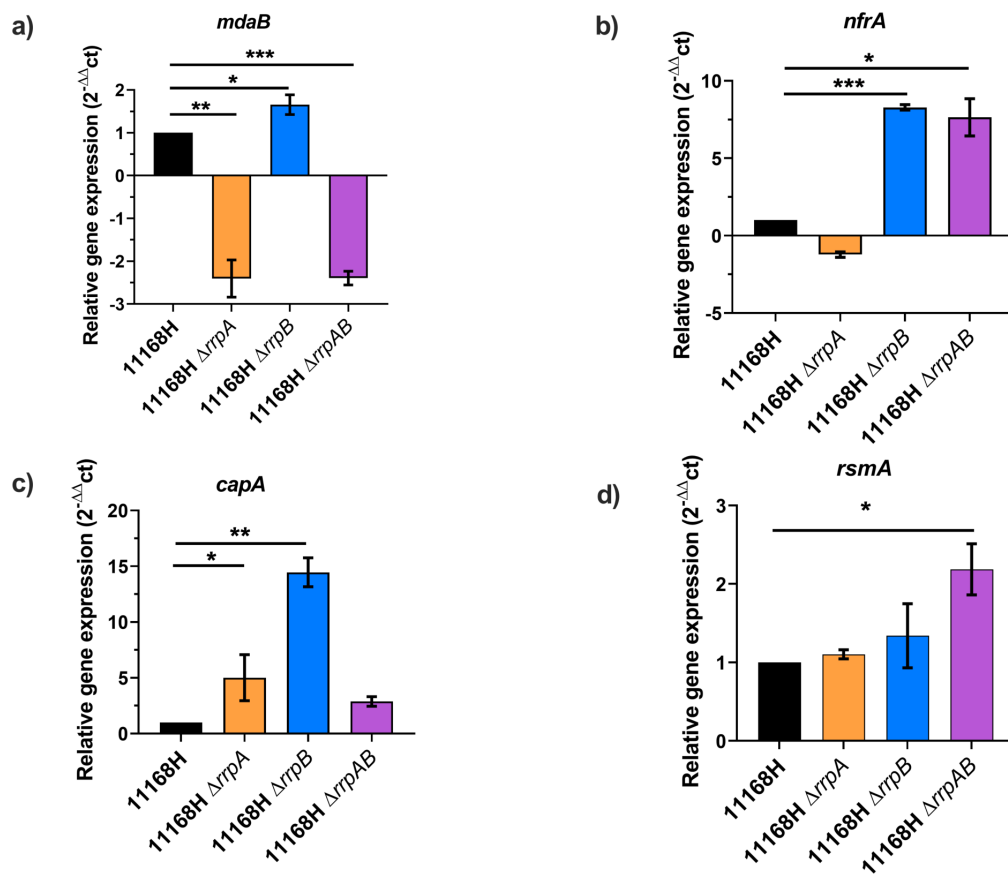


Figure 2:

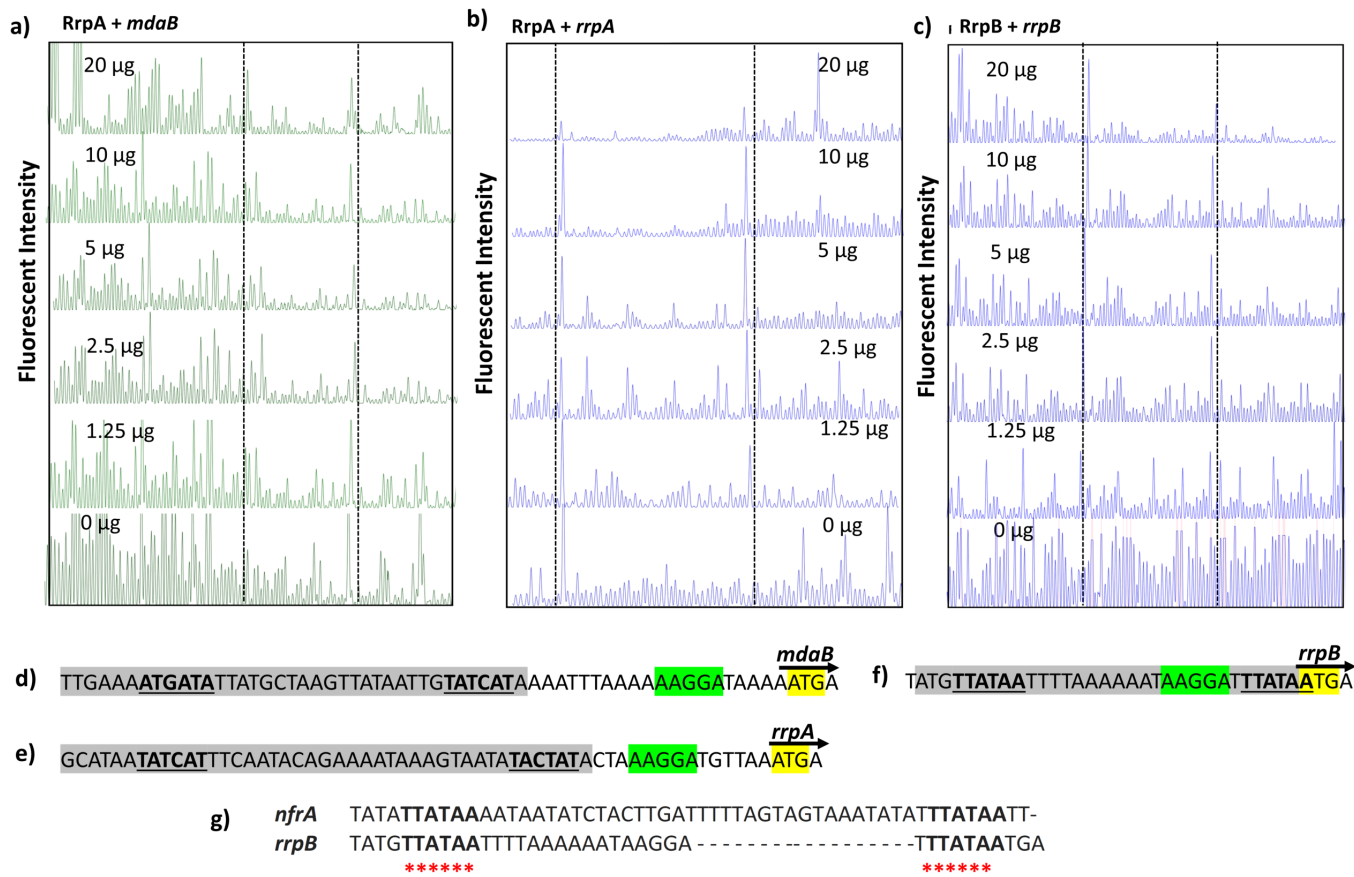


Figure 3:

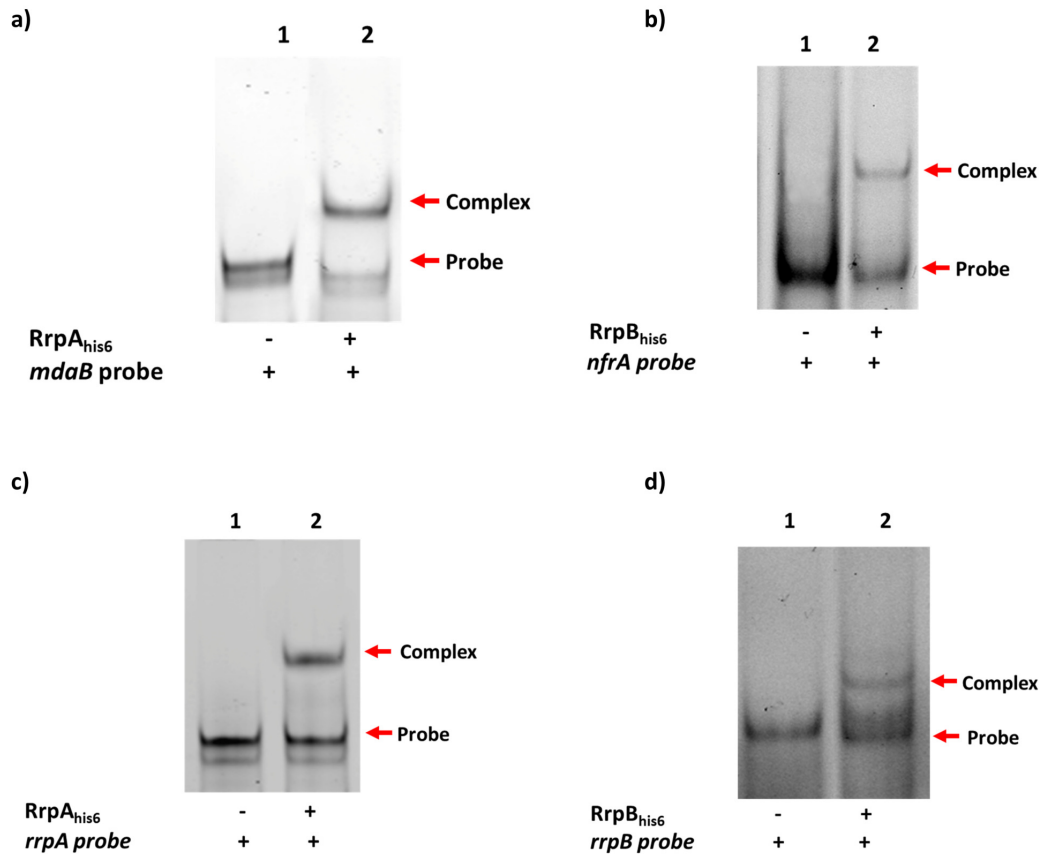


Figure 4:

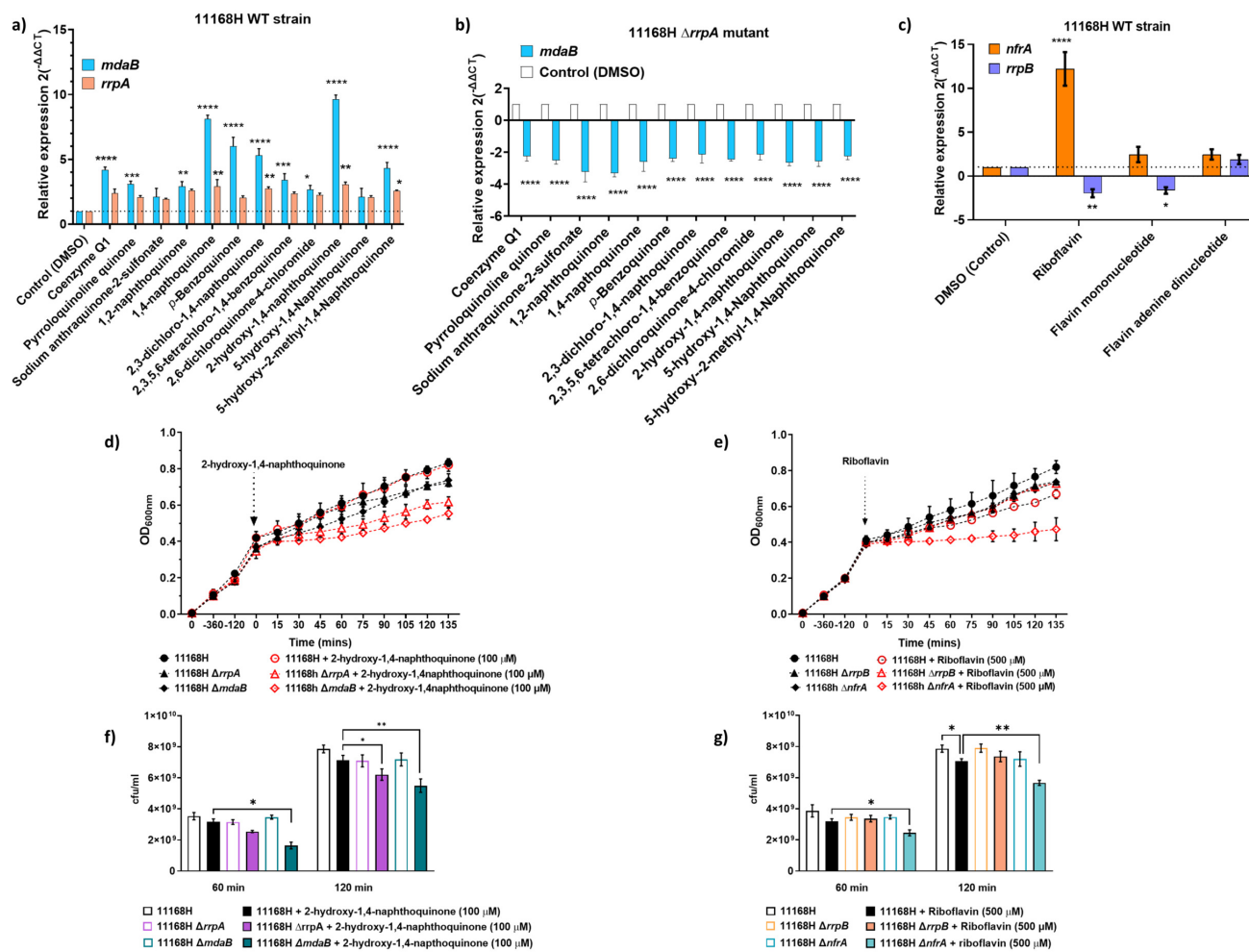


Figure 5:

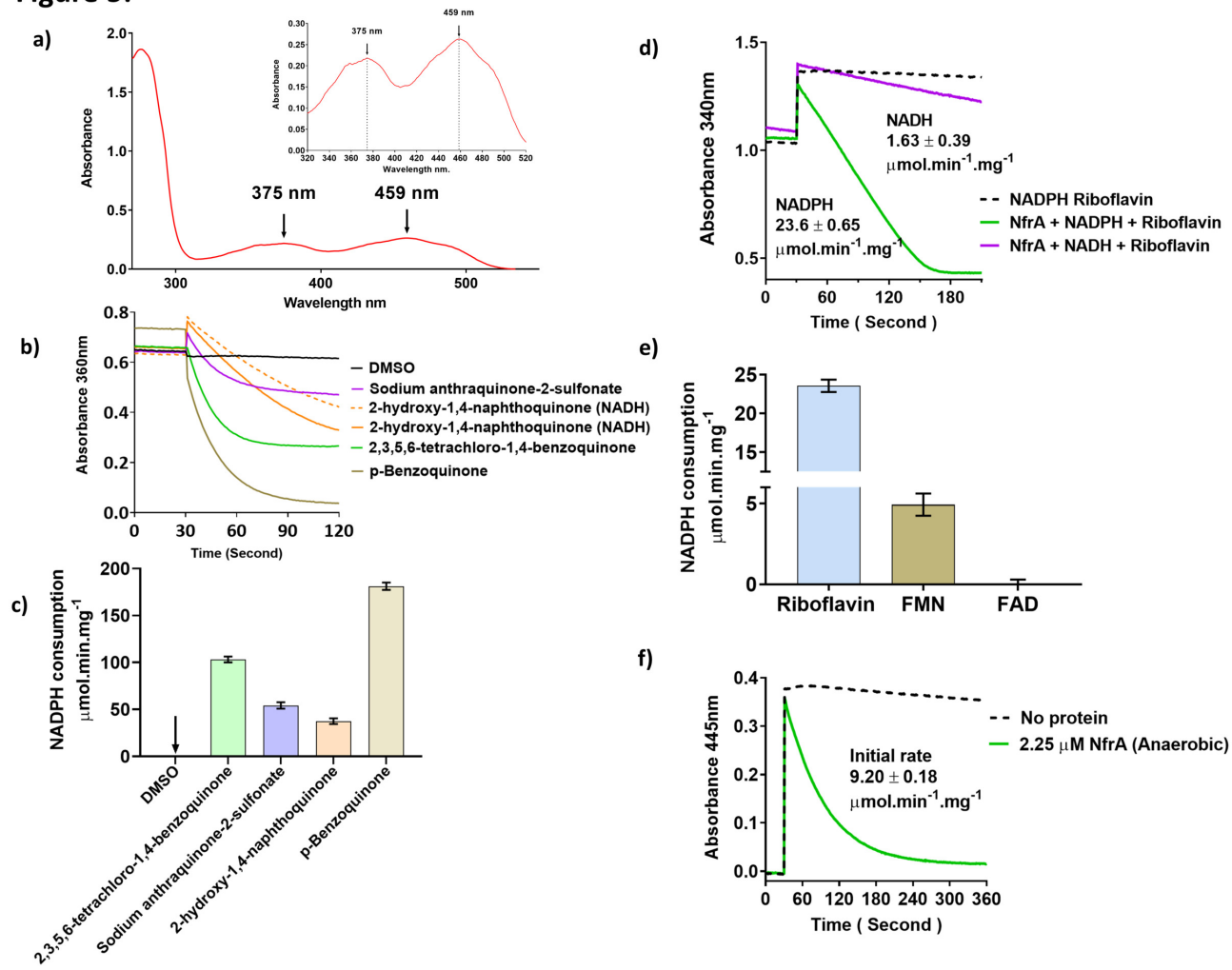


Figure 6:

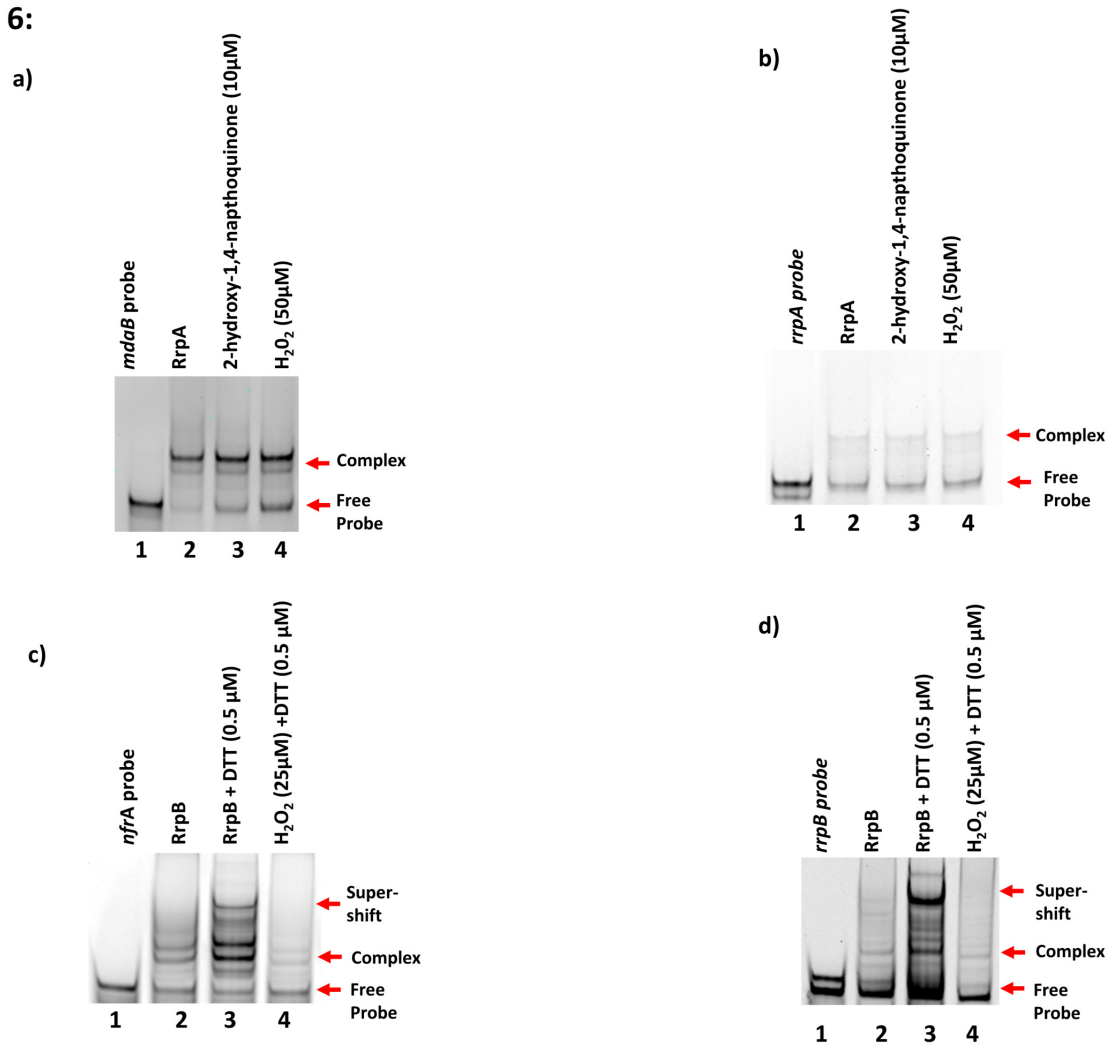


Figure 7:

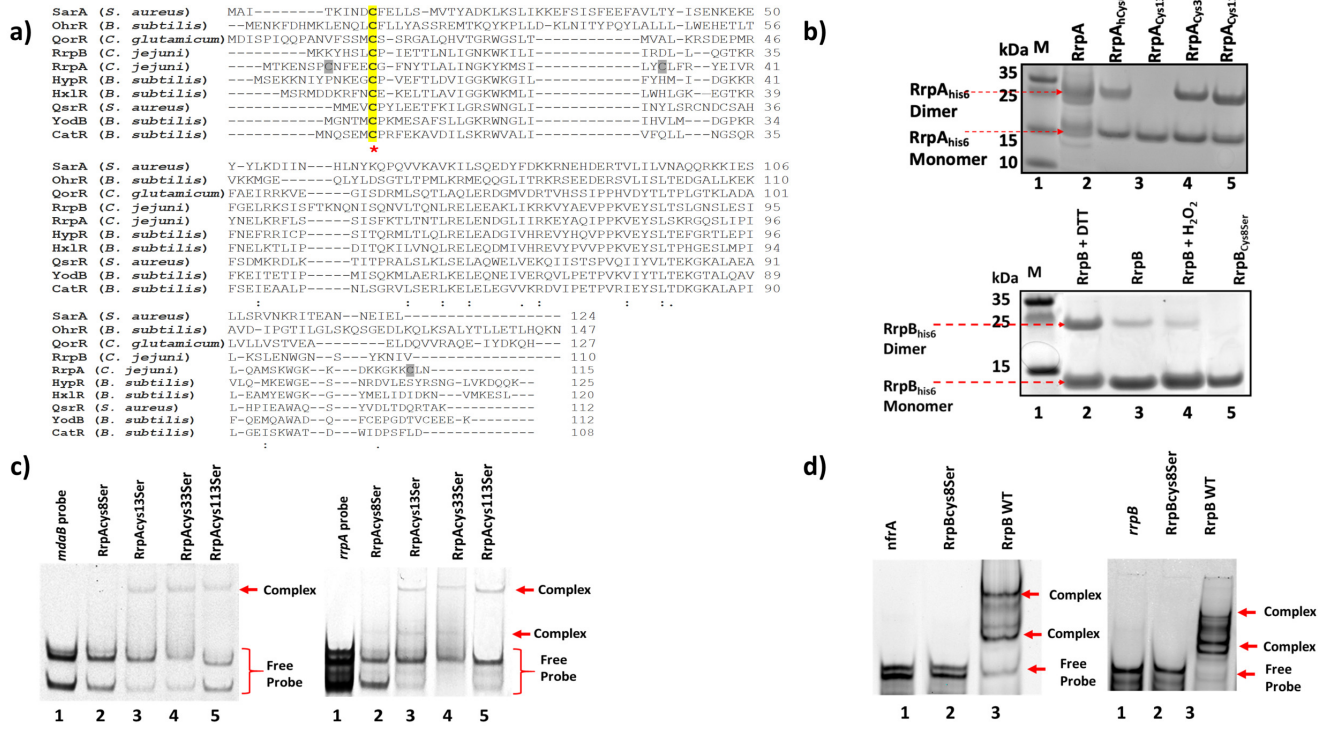
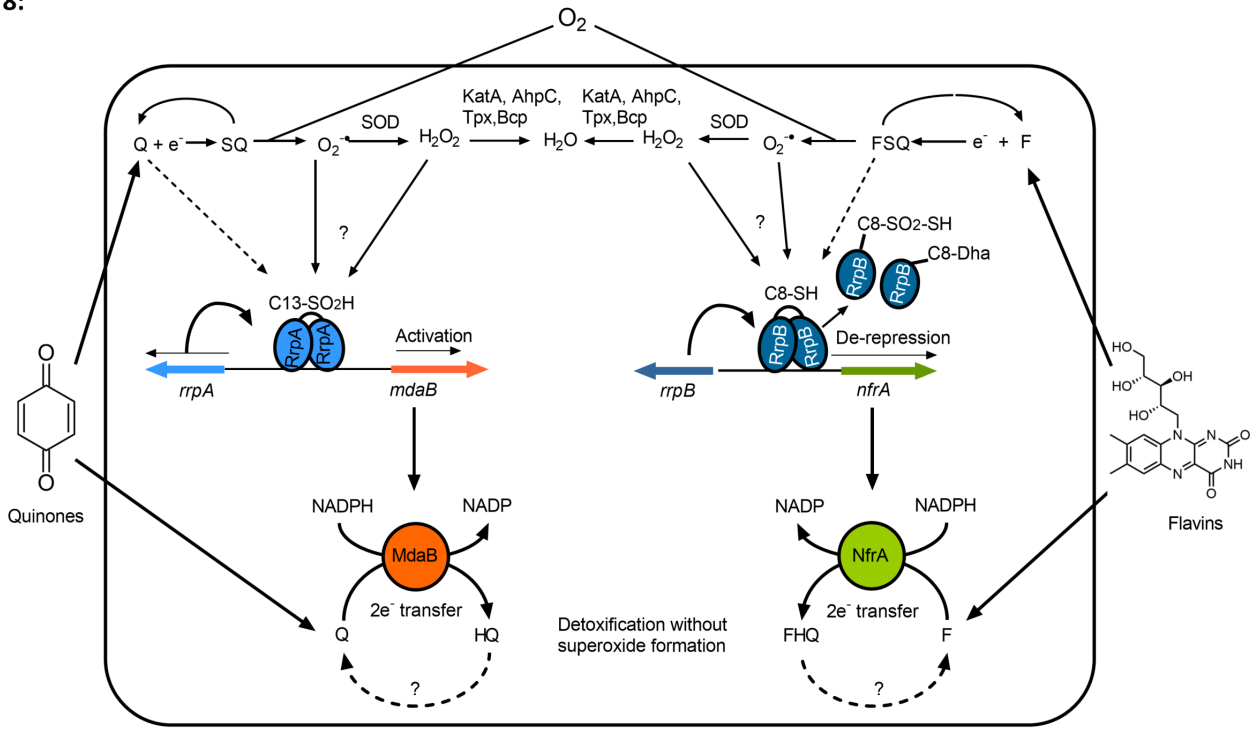


Figure 8:



1 **MdaB and NfrA, two novel reductases important in the survival and**
2 **persistence of the major enteropathogen *Campylobacter jejuni***

3

4 **Running title:** MdaB and NfrA Aid Survival of *C. jejuni*

5

6 Fauzy Nasher^{1*}, Aidan J. Taylor², Abdi Elmi¹, Burhan Lehri¹, Umer Z. Ijaz³, Dave Baker⁴,
7 Richard Goram⁵, Steven Lynham⁶, Dipali Singh⁴, Richard Stabler¹, David J. Kelly², Ozan
8 Gundogdu¹, Brendan W. Wren^{1*}.

9

10 ¹Faculty of Infectious and Tropical Diseases, London School of Hygiene and Tropical
11 Medicine, London, United Kingdom.

12 ²Department of Molecular Biology and Biotechnology, University of Sheffield, Sheffield,
13 United Kingdom.

14 ³School of Engineering, University of Glasgow, Glasgow, United Kingdom

15 ⁴Microbes in Food Chain, Quadram Institute Biosciences, Norwich Research Park, Norwich,
16 United Kingdom.

17 ⁵The John Innes Centre, Norwich Research Park, Norwich, United Kingdom

18 ⁶Proteomics Facility, Centre of Excellence for Mass Spectrometry, King's College London,
19 London, United Kingdom.

20

21 *Address correspondence to **Brendan W. Wren**, brendan.wren@lshtm.ac.uk
22 and **Fauzy Nasher**, fauzy.nasher1@lshtm.ac.uk

23

24

25

26

27

28

29 **Abstract**

30 The paralogues RrpA and RrpB which are members of MarR family of DNA binding proteins
31 are important for the survival of the global bacterial foodborne pathogen *Campylobacter*
32 *jejuni* under redox stress. We report that RrpA is a positive regulator of *mdaB*, encoding a
33 flavin-dependent quinone reductase that contributes to the protection from redox stress
34 mediated by structurally diverse quinones, whilst RrpB negatively regulates the expression of
35 *cj1555c* (renamed *nfrA* for NADPH-flavin reductase A), encoding a flavin reductase. NfrA
36 reduces riboflavin at a greater rate than its derivatives, suggesting exogenous free flavins are
37 the natural substrate. MdaB and NfrA both prefer NADPH as an electron donor. Cysteine
38 substitution and post-translational modification analyses indicated that RrpA and RrpB
39 employ a cysteine-based redox switch. Complete genome sequence analyses revealed *mdaB*
40 is frequently found in *Campylobacter* and related *Helicobacter spp.*, whilst *nfrA* is
41 predominant in *C. jejuni* strains. Quinones and flavins are redox cycling agents secreted by a
42 wide range of cell-types that can form damaging superoxide by one-electron reactions. We
43 propose a model for stress adaptation where MdaB and NfrA facilitate a two-electron
44 reduction mechanism to the less toxic hydroquinones, thus aiding survival and persistence of
45 this major pathogen.

46

47 **Importance**

48 Changes in cellular redox potential results in alteration in the oxidation state of intracellular
49 metabolites and enzymes, consequently, cells make adjustments that favor growth and
50 survival. The work we present here answers some of the many questions that have remained
51 elusive over the years of investigation into the enigmatic microaerophile bacterium,
52 *Campylobacter jejuni*. We employed molecular approaches to understand the regulation
53 mechanisms and functional analyses to reveal the roles of two novel quinone and flavin

54 reductases, both serve as major pools of cellular redox-active molecules. This work extends
55 our knowledge on bacterial redox sensing mechanisms and the significance of hemostasis.

56

57 **Introduction**

58 *Campylobacter jejuni* is a microaerophilic Gram-negative bacterium and is the leading cause
59 of bacterial foodborne gastroenteritis worldwide (1). The high prevalence of *C. jejuni* is
60 accredited to its ability to survive in a variety of niches including the natural environment and
61 within its avian and mammalian hosts, despite not growing in aerobic environments (2).

62

63 The sensitivity of *C. jejuni* to both oxygen and oxidative stress is a major defining feature
64 that has presented a conundrum in terms of the prevalence of the bacterium in the natural
65 environment and its success as a global enteric pathogen. Genomic data, mutant phenotypes
66 and biochemical analyses have shown that *C. jejuni* strains have an extensive complement of
67 oxidative stress protection systems (3), that allows fine tuning of its adaptation to *in vivo* and
68 *ex vivo* environments. These include the peroxidatic enzyme catalase and the thiol
69 peroxidases Tpx, Bcp and AhpC as well as superoxide dismutase (4, 5).

70

71 The production of most of the above mentioned oxidative stress protection enzymes are
72 controlled at the transcriptional level by the regulators PerR, CosR and Fur (3). However, the
73 re-annotation of the *C. jejuni* NCTC 11168 genome led to the discovery of two novel redox-
74 sensing MarR-homologue transcriptional regulators that were named RrpA (*cj1546*) and
75 RrpB (*cj1556*) (6, 7). Using *C. jejuni* 11168H, a hypermotile derivative of the standard strain
76 NCTC 11168 (8, 9), a link between RrpA and RrpB with oxidative stress was reported based
77 on decreased viability in mutant strains after treatment with oxidative stress inducing

78 compounds, hydrogen peroxide, menadione and cumene hydroperoxide (6, 7, 10).
79 Additionally, multilocus sequencing typing (MLST) revealed that *rrpA* was present in over
80 99% of 3,746 *C. jejuni* strains, but the presence of *rrpB* predominated in livestock-associated
81 strains (10). This suggests a correlation between possession of both transcriptional regulators
82 and the ability of *C. jejuni* to adapt and survive in diverse niches.

83

84 Here, we asked what genes are under the regulatory control of RrpA and RrpB and what their
85 roles are in *C. jejuni* redox metabolism. We identified *mdaB* and *nfrA*, encoding two novel
86 reductases that are under the transcriptional control of RrpA and RrpB, respectively, and we
87 revealed the regulation mechanism of RrpA and RrpB to their DNA substrates. We show
88 MdaB is a flavin-dependent NADPH-quinone reductase, which has a role in protecting the
89 cell from quinone stress mediated damage, while NfrA is an NADPH-riboflavin reductase.
90 Database searches revealed that MdaB is predominant in both *Campylobacter spp.* and the
91 related *Helicobacter spp.*, but NfrA is more often found in *C. jejuni* strains commonly
92 associated with human infection.

93

94 Quinones are amongst the main chemical compounds produced by plants and
95 microorganisms and have attracted significant interest because of their antimicrobial
96 activities (11). Quinones are well known for their active role in the electron transport chain of
97 most organisms in the form lipid-soluble electron carriers (e.g., ubiquinone and
98 menaquinones) (12). In contrast, water-soluble quinones are toxic as pro-oxidants or
99 electrophiles (13-16), and act as catalysts to generate reactive oxygen species (ROS) by
100 undergoing one-electron reduction to yield semi-quinone radical anions that reduce molecular
101 oxygen. This produces ROS such as the superoxide anion ($O_2^{\bullet-}$) and hydrogen peroxide
102 (H_2O_2) that lead to redox cycling reactions (17, 18).

103

104 Flavin mononucleotide (FMN) and flavin dinucleotide (FAD), and rarely riboflavin itself,
105 form an integral part of the redox active sites of flavoproteins as prosthetic groups (19). The
106 core of flavin compounds consist of a heterocyclic isoalloxazine ring that exist in three
107 different redox states: oxidized form, one-electron reduced radical semiquinone and two-
108 electron fully-reduced hydroquinone (20). In fact, this property makes flavin molecules
109 unique compounds in nature and fit to serve in broad roles as biocatalysts. However, similarly
110 to quinones, flavo-semiquinones can transfer an electron to oxygen generating the superoxide
111 radical (16, 21). Additionally, free flavins have been shown to transfer electrons to convert
112 Fe^{3+} into Fe^{2+} and O_2 into H_2O_2 . The simultaneous production of H_2O_2 and Fe^{2+} in cells may
113 promote the production of hydroxyl radical via the Fenton reaction resulting in cell death
114 (22).

115

116 Given their propensity for highly toxic superoxide production, both quinones and flavins are
117 effective antimicrobials (23, 24) that *C. jejuni* may encounter in *in vivo* and *ex vivo*
118 environments. Thus, we propose that possession of the MdaB and NfrA enzymes allows a
119 safer two-electron reduction to the fully reduced forms of these compounds and could be a
120 significant adaptation for the persistence and prevalence of this problematic pathogen.

121

122 **Results**

123 **Disruption of *rrpA*, *rrpB* and *rrpAB* shows altered transcription profiles in *C.***

124 ***jejuni* 11168H.**

125 The pleiotropic phenotype of the *C. jejuni* $\Delta rrpA$, $\Delta rrpB$ and $\Delta rrpAB$ strains (6, 7, 10), led us
126 to examine the transcription profiles of the 11168H wild type and its respective $\Delta rrpA$, $\Delta rrpB$

127 and $\Delta rrpAB$ defined mutants by RNA-Seq. Bacteria were cultured in brucella broth at 37 °C
128 in microaerobic condition to $OD_{600nm} = \sim 0.45$ (mid-log growth phase), five biological
129 replicates were analyzed. Genes that were significantly differentially regulated between the
130 wild type and mutant strains are presented in **Table 1** (genes that were differentially
131 expressed $>1.5 \log^2$ fold change compared to the wild type were considered significant;
132 $p < 0.05$).

133

134 There was a modest difference in gene expression between the wild type strain and its $\Delta rrpA$
135 or $\Delta rrpB$ mutants; the putative autotransporter gene *capA* (*cj1677*), was significantly
136 upregulated in both the $\Delta rrpA$ and $\Delta rrpB$ mutants (**Table 1**). RrpB was previously reported to
137 be an autoregulator (6), and interestingly, in both $\Delta rrpB$ and the $\Delta rrpAB$ mutant strains, *rrpB*
138 and the gene directly upstream on the reverse strand, *cj1555c*, were significantly upregulated
139 (**Table 1**). *cj1555c* codes for a hypothetical protein of unknown function, however, a protein
140 BLAST search (<https://blast.ncbi.nlm.nih.gov/>) indicated that this gene is an NAD(P)H-
141 flavin reductase, which we have named *nfrA*, NAD(P)H-flavin reductase A.

142

143 Additionally, in the $\Delta rrpA$ mutant, *cj1545c* (*mdaB*; modulator of drug activity B) was
144 downregulated based on individual statistical test ($p < 0.05$), however, when the *p*-values were
145 adjusted for multiple comparison, the significance was lost. Nevertheless, this gene was
146 included in the study (indicated with an asterisk * in **Table 1**), for two reasons: 1). *mdaB* was
147 previously implicated to have a role in oxidative stress defense in *C. jejuni* and in the closely
148 related *Helicobacter spp.* (25, 26); and 2). *mdaB* is located directly upstream of *rrpA* on the
149 reverse strand in a divergent orientation.

150

151 In the double mutant strain, $\Delta rrpAB$, genes that were significantly upregulated included *rrpA*;
152 which was previously also reported to be an autoregulator (7); *cj1719c* which encodes LeuA
153 (2-isopropylmalate synthase), an amino acid biosynthesis protein; *cj1454c*, encoding RimO, a
154 ribosomal methylthiotransferase that catalyzes the methylthiolation of aspartic acid residue of
155 ribosomal protein S12; *cj1710c*, encoding Rnj, involved in the maturation and/or decay of
156 mRNA; and *cj1711c*, encoding RsmA, which plays a role in the biogenesis of ribosomes and
157 has been shown to protect DNA against oxidative stress in some bacteria (27, 28). Two genes
158 were significantly downregulated, *cj0724*; which is an uncharacterized molybdenum cofactor
159 biosynthesis protein and *cj0265c*; the TorB cytochrome *c*-type heme-binding subunit of the
160 TorAB, TMAO/DMSO reductase (**Table 1**). Tables of all genes are presented in **Table. S1a**,
161 **Table. S1b and Table. S1c**.

162
163 RNA independent from the RNA-Seq was isolated and real-time RT-qPCR was performed
164 (**Fig. 1**). RT-qPCR indicated a significant ~2-fold decrease in the expression of *mdaB* in both
165 $\Delta rrpA$ and $\Delta rrpAB$ mutant strains, whilst in the $\Delta rrpB$ mutant strain, *mdaB* was significantly
166 upregulated by ~1.5-fold (**Fig.1a**). In both $\Delta rrpB$ and $\Delta rrpAB$ mutant strains, *nfrA* was
167 significantly upregulated by ~7-fold (**Fig.1b**). Expression of *capA* and *rsmA* were also
168 confirmed in all the strains, and their expressions were in line with our RNA-Seq data (**Fig.**
169 **1c and 1d**).

170
171 Our RNA-Seq and RT-qPCR results showed the genes located upstream of *rrpA* and *rrpB*,
172 respectively, were differentially regulated in the mutant strains. Therefore, we speculated that
173 these genes are under the control of RrpA and RrpB. DNase I footprinting using dye primer
174 sequencing on an automated capillary DNA analysis system was used to test the interactions

175 of recombinant RrpA_{his6} and RrpB_{his6} proteins with the regions upstream of the genes *mdaB*
176 and *nfrA*.

177

178 **RrpA and RrpB protect regions with inverted repeat sequences.**

179

180 DNase 1 footprinting was performed as described previously (29), a 500 ng fluorescently
181 labelled DNA fragment was incubated with various concentrations of recombinant RrpA_{his6}
182 and RrpB_{his6} ranging from 20 µg to 0 µg at room temperature, as described in the Methods.

183 The pattern of protection was observed by decreased fluorescent intensity of the
184 electropherogram (indicated within the dotted lines) (**Fig. 2**). We also noted non-specific
185 protection patterns at the highest protein concentrations in all of the samples, possibly due to
186 promiscuity at high protein concentrations due to low binding affinity.

187

188 We observed protection by purified RrpA_{his6} upstream of *mdaB* and upstream of the *rrpA*
189 translational start sites (**Fig. 2a** and **Fig. 2b**), respectively. Purified RrpB_{his6} showed
190 protection upstream of the *rrpB* translational start site (**Fig. 2c**). In these protected regions
191 (highlighted in grey), we identified inverted repeats (IRs) motif (underlined in bold) protected
192 by RrpA_{his6} formed by 6 nt (5'-TATCAT-3'), which are separated by 19 nt for *mdaB* (**Fig. 2d**)
193 and 24 nt for *rrpA* (**Fig 2e**), we also identified an IR sequence protected by RrpB_{his6} formed
194 of 6 nt (5'-TTATAA-3') separated by 17 nt (**Fig. 2f**). We did not observe protection by
195 RrpB_{his6} upstream of *nfrA*, possibly due to oxidation of the protein during sample preparation.
196 However, nucleotide alignment of the region preceding the translation start site of *nfrA*
197 identified IR sequence that matched those found within the protected region by RrpB_{his6},
198 upstream of the translation site of *nfrA* (**Fig. 2g**).

199

200 Oligonucleotides spanning the protected regions were synthesized and Electrophoretic
201 Mobility Shifts Assays (EMSA) were conducted. A DNA substrate, 50 nM, was co-
202 incubated with final concentration of 0.05 μ g of RrpA_{his6} and RrpB_{his6} proteins in a 20 μ l
203 reaction; formation of protein-DNA complexes were observed in all the EMSAs conducted
204 (**Fig. 3a-d**) Specificity of binding was also tested, we found that both RrpA_{his6} and RrpB_{his6}
205 proteins are able to bind to DNA sequences with mutation to one of the binding sequences
206 but were unable to bind to DNA that lack both binding sequences (**Fig. S1a and Fig. S1b**).
207 This is indicative that RrpA and RrpB recognize regions on the DNA with IR sequences,
208 which is characteristic of the MarR family transcriptional regulators (30).

209

210 ***mdaB-rrpA* and *nfrA-rrpB* gene expression respond to a range of exogenous**
211 **quinones and flavins, respectively.**

212

213 We performed a literature search to identify broad range of quinones that have previously
214 been shown to have an effect on *mdaB* analogs (25, 31). We selected the following
215 compounds due to their structural diversity; Coenzyme Q1 (Ubiquinone), Pyrroloquinoline
216 quinone (Methoxatin), Sodium anthraquinone-2-sulfonate, 1,2-Naphthoquinone (Ortho-
217 naphthoquinone), 1,4-naphthoquinone, p-Benzoquinone, 2,3-dichloro-1,4-naphthoquinone
218 (Dichlone), 2,3,5,6-tetrachloro-1,4-benzoquinone (Chloranil), 2,6-dichloroquinone-4-
219 chloromide (Gibb's reagent), 2-hydroxy-1,4-naphthoquinone (Lawsone), 5-hydroxy-1,4-
220 Naphthoquinone (Juglone), 5-hydroxy--2-methyl-1,4-Naphthoquinone (Plumbagin). We also
221 tested gene expression of *nfrA* and *rrpB* in response to riboflavin and its derivatives, flavin
222 mononucleotide (FMN) and flavin dinucleotide (FAD). Growing cultures of *C. jejuni* 11168h
223 and its mutants (mid-log OD_{600nm} = ~0.45) were treated with the compounds and gene

224 expression at 15 mins and 40 mins was determined by RT-qPCR relative to the control after
225 normalization using *gyrA* (**Fig. 4**).

226

227 In the wild-type strain the expression of *mdaB* and *rrpA* were greatly influenced by treatment
228 with quinone compounds. The greatest effect was observed after treatment with 2-hydroxy-
229 1,4-naphthoquinone; *mdaB* expression was increased by ~9.6-fold and *rrpA* by ~3.0-fold
230 after 15 mins (**Fig. 4a**) and *mdaB* expression remained significantly high (~5-fold) after 40
231 mins post treatment (**Fig. S2a**). Interestingly, the expression of *mdaB* was significantly
232 reduced (~3.0-fold) in the $\Delta rrpA$ mutant strain at 15 mins (**Fig. 4b**) and 40 mins (**Fig. S2b**).

233 Similarly, treatment of *C. jejuni* 11168H with exogenous flavins showed *nfrA* gene
234 expression was significantly increased up to ~12-fold after 15 mins of treatment, whilst *rrpB*
235 expression was significantly reduced (~2-fold) (**Fig. 4c**). *nfrA* expression remained
236 significantly high after 40 mins post-treatment with riboflavin and FMN (**Fig. S2c**). These
237 results also suggest that *mdaB* and *nfrA* are under the regulatory control of RrpA and RrpB,
238 respectively.

239

240 Given that 2-hydroxy-1,4-naphthoquinone and riboflavin had an effect on *mdaB-rrpA* and
241 *nfrA-rrpB* expressions, respectively, we tested their effects on *C. jejuni* growing cultures;
242 Optical density (OD_{600nm}) was monitored for 135 mins after the addition of 100 μ M 2-
243 hydroxy-1,4-naphthoquinone (**Fig. 4d**) and 500 μ M of riboflavin (**Fig. 4e**). Addition of 2-
244 hydroxy-1,4-naphthoquinone led to a temporary bacteriostatic effect and reduction in
245 maximum optical density of strain $\Delta rrpA$, $\Delta rrpAB$ and $\Delta mdaB$ compared to wild type (**Fig.**
246 **4d**), the addition of riboflavin had a modest effect on the wild type strain but the largest effect
247 was observed on $\Delta nfrA$ mutant strain. As OD can be affected by cell morphology, we also
248 determined viability by colony forming units (cfu) at 60 mins and 120 mins after treatment

249 with 2-hydroxy-1,4-naphthoquinone (**Fig. 4f**) or riboflavin (**Fig. 4g**). These results were in
250 line with the optical density measurements. We did not observe any effect on the *nfrA* mutant
251 strain at a lower concentration (100 μ M) of riboflavin.

252

253 **MdaB and NfrA reduce quinones and flavins, respectively.**

254

255 We conducted a conserved-domain search on the *C. jejuni* MdaB and NfrA proteins, MdaB
256 contains a flavodoxin-like fold ([C100438](#)), whilst NfrA is a member of a large family that
257 share a Rossmann-fold NAD(P)H/NAD(P)(+) binding (NADB) domain ([C121454](#)). MdaB
258 and NfrA were predicted to be a putative NAD(P)H-quinone reductase and NAD(P)H-flavin
259 reductase, respectively; we therefore tested the reductase activity of purified recombinant *C.*
260 *jejuni* MdaB and NfrA in the presence of quinones and flavins (riboflavin, FMN and FAD),
261 respectively. Purified MdaB_{his6} showed a flavin absorption spectrum with peaks at 454 nm
262 and 379 nm, characteristic of a FAD/FMN cofactor protein (**Fig. 5a**). The isoalloxazine ring
263 system within flavins generates a yellow color that is also responsible for light absorption in
264 the UV and visible spectral range such as that observed for MdaB_{his6} (25, 32, 33). The
265 reductase activity of MdaB was determined by monitoring the oxidation of NADPH in the
266 presence of quinone substrates. Specific activities were determined in the range of 37 to 181
267 μ mol min⁻¹ mg⁻¹ protein (**Fig. 5b and Fig. 5c**). Note that due to interference of substrates at
268 340 nm, 360 nm was used in these assays and the extinction coefficient for NADPH at 360
269 nm was determined as 4.61 l mmol⁻¹ cm⁻¹. We also found that MdaB had NADPH oxidase
270 activity under atmospheric oxygen conditions, therefore all assays were performed
271 anaerobically (**Fig. S3a**). Some of the quinones tested were incompatible with the assay, due
272 to insolubility in aqueous buffer (**Fig. S3b**), scans of all the quinone compounds tested (**Fig.**
273 **S3c**) and controls (**Fig. S3d**) are presented in supplementary file S1.

274

275 The flavin reductase activity of NfrA was determined by measuring the oxidation of
276 NAD(P)H in the presence of the flavin substrates riboflavin, FMN and FAD. The specific
277 activity with riboflavin was determined as 23.6 and 1.63 $\mu\text{mol min}^{-1} \text{mg}^{-1}$ protein with
278 NADPH and NADH as electron donor, respectively. This was indicative of NfrA preference
279 for NADPH over NADH (**Fig. 5d**). NfrA dependent reduction of FMN and FAD with
280 NADPH was also determined. NfrA had some activity towards FMN (4.9 $\mu\text{mol min}^{-1} \text{mg}^{-1}$,
281 4.8-fold lower than riboflavin) but no significant activity with FAD (**Fig. 5e and Fig. S3e**).
282 Riboflavin reduction by NfrA in the presence of NADPH was monitored directly by
283 performing the assay anaerobically and following the absorbance maximum of riboflavin
284 (445nm). A specific activity of 9.20 $\mu\text{mol min}^{-1} \text{mg}^{-1}$ protein was calculated from the
285 determined extinction coefficient for riboflavin at 445nm of 2.13 l $\text{mmol}^{-1} \text{cm}^{-1}$ (**Fig. 5f**). No
286 activity was detected with either NAD^+ or NADP^+ (**Fig. S3f**). Spectra scans performed pre-
287 and post- assay to confirm quantitative reduction of riboflavin are presented in supplementary
288 file S1 (**Fig. S3g**).

289

290 **RrpA_{his6} and RrpB_{his6} are post-translationally modified *in vitro* by treatment with**
291 **redox cycling agents**

292

293 MarR-like transcription regulators utilize a redox sensing cysteine (Cys) residue “redox-
294 switch” for their activity. We hypothesized that the same mechanism is employed by RrpA
295 and RrpB. Protein sequence analysis revealed that RrpA has four Cys residues (Cys8, Cys13,
296 Cys33 and Cys113) and RrpB has one Cys residue (Cys8) within the protein.

297

298 We tested the effects of redox cycling compounds on recombinant RrpA_{his6} and RrpB_{his6}
299 binding to their DNA substrates by EMSA (**Fig. 6**). Treatment of RrpA_{his6} with 10 μ M of 2-
300 hydroxy-1,4-naphthoquinone or 50 μ M H₂O₂ did not affect its ability to form a complex with
301 its DNA substrates; *mdaB* (**Fig. 6a**) and *rrpA* (**Fig. 6b**). Our RNA-Seq and RT-qPCR results
302 indicated that RrpB is a negative regulator of *nfrA* and *rrpB*, considering that the environment
303 within the cell is maintained in a reduced state, EMSAs were performed in the presence of a
304 reducing agent (dithiothreitol (DTT)) to mimic this condition *in vitro*. Interestingly, RrpB_{his6}
305 formed a higher complex (super-shift) with its substrates in the presence of DTT (**Fig. 6c and**
306 **6d**) and the addition of 25 μ M of H₂O₂ attenuated this protein–DNA complex (**Fig. 6c and**
307 **6d**). This suggested that the de-repression mechanism of RrpB is mediated by redox
308 compounds.

309

310 We investigated whether RrpA and RrpB Cys residues are modified after treatment with
311 redox compounds, *in vitro*. Recombinant proteins were incubated with 50 μ M of 2-hydroxy-
312 1,4-naphthoquinone or H₂O₂ on RrpA_{his6} and H₂O₂ on RrpB_{his6} at room temperature for 30
313 mins and the proteins were analyzed by liquid chromatography mass spectrometry (LC-
314 MS/MS). Total ion current (TIC) of the peptides was used to compare the treated samples to
315 the untreated samples (**Table. 2**).

316

317 Analysis of RrpA_{his6} treated with 2-hydroxy-1,4-naphthoquinone or H₂O₂ showed a peptide
318 with a mass peak of 2460.1 Da and an m/z of 821.03³⁺, an assigned loss of 34 Da was
319 detected on Cys8, corresponding to a dehydroalanine (Dha) modification and the second
320 modification was assigned with the addition of 32 Da, a di-oxidation (Sulfinic acid (Cys-
321 SO₂H)) of Cys 13. A doubly-charged peptide with a mass peak of 1110.6 Da and an m/z of
322 556.30²⁺ was also detected in RrpA_{his6} treated with 2-hydroxy-1,4-naphthoquinone, this

323 peptide contained a single Cys residue with a matched loss of 34 Da, confirmed as a Dha
324 modification on Cys33. RrpA_{his6} treated with H₂O₂ showed a peptide with a mass peak of
325 1126.6 Da and an m/z of 564.30²⁺, which was confirmed as a Dha modification on Cys33 and
326 a single oxidation on Met28. Dha is a desulphurization event with the potential to destabilize
327 protein three-dimensional structure by disruption of disulfide bond formation (34). Sulfinic
328 acid (Cys-SO₂H) is stable and forms disulfide bonds with nearby Cys thiol groups, mediated
329 by ROS and oxidants, both Dha and sulfinic acid modifications are reversible (35). Cys113 in
330 RrpA_{his6} was not matched as the tryptic peptide contained only three residues and was below
331 the lower mass-to-charge fragmentation window set in the MS method.

332

333 Analysis of RrpB_{his6} treated with H₂O₂ identified a peptide with a mass peak of 1978.95 Da
334 and an m/z of 990.48²⁺. This was identified as an addition of 64 Da and confirmed as an
335 irreversible (35) sulfur dioxide modification (Thiosulfonic acid (Cys-SO₂-SH)) at Cys8.
336 Thiosulfonic acid results from over-oxidation of Cys and is a unique byproduct of degraded
337 Cys-S-SO₂-Cys. Degradation of this disulfide bond also produces a Dha modified cysteine
338 (**Fig. S4**).

339

340 Modifications to peptides in the untreated samples were also detected, possibly generated
341 upon sample preparation. PTM peptides with a lower TIC relative to the control were also
342 detected in the treated samples, as well as possible undesired non-functional amino acids. A
343 full identification table and peptide intensity values are presented in **Table. S2**.

344

345 Sequence alignment (36) to other MarR family transcription regulators revealed conserved
346 Cys residues in RrpA, Cys13, and RrpB, Cys8 (**Fig. 7a**). To explore the role of Cys residues
347 in RrpA and RrpB further, we generated variants by substituting Cys with serine; RrpA_{Cys8Ser},

348 RrpA_{Cys13Ser}, RrpA_{Cys33Ser}, RrpA_{Cys113Ser} and RrpB_{Cys8Ser}. Non-reducing SDS-PAGE was used
349 to analyze migration of RrpA_{his6}, RrpB_{his6} and their variants. RrpA_{his6} and its variants with the
350 exception of RrpA_{Cys13Ser} migrated at the size of RrpA dimer (**Fig. 7b**). RrpB_{his6} reduced (0.5
351 μ M DTT) also migrated at the size of RrpB dimer, however, RrpB_{his6} oxidized (50 μ M H₂O₂)
352 and RrpB_{Cys8Ser} both migrated at the size of a monomer (**Fig. 7b**). These results indicate that
353 the conserved Cys residues in both proteins are critical for the dimeric forms.

354

355 The ability of RrpA_{his6} and RrpB_{his6} variants to bind DNA substrates was tested by EMSA.
356 All RrpA variants were able to form protein-DNA complexes (**Fig. 7c**), with the exception of
357 the non-conserved RrpA_{Cys8Ser}. Similarly, RrpB mutation to the conserved sole Cys residue
358 Cys8 resulted in the inability of RrpB_{Cys8Ser} to form protein-DNA complexes (**Fig. 7d**).

359

360 Discussion

361 We have unraveled the roles of two novel reductases, MdaB (modulator of drug activity B)
362 and NfrA (Cj1555c), that contribute to the survival and persistence of *C. jejuni*. *mdaB* and
363 *nfrA* are under the control of RrpA and RrpB, respectively, which are members of the MarR
364 family of DNA binding proteins. RrpA is highly conserved among *C. jejuni* strains, whilst
365 RrpB is predominant in the livestock-associated MLST clonal complex (10, 37), and are
366 prevalent in strains isolated from humans. In other organisms including *Helicobacter spp.*,
367 MdaB is a flavin-dependent NADPH-quinone reductase that has been suggested to fully
368 reduce quinones and subsequently prevents the generation of the highly reactive
369 semiquinones (38-40). NfrA is a NADPH-flavin reductase, and in other bacteria, flavin
370 reductases have been shown to have a role in iron bioavailability and maintain a supply of
371 flavin cofactors to proteins involved in cell homeostasis (41), but given that flavins are also

372 redox active and the control of *nfrA* by the redox responsive regulator RrpB, it seems more
373 likely that NfrA reduces flavins, this potentially prevents generation of toxic semiquinones.

374

375 Organisms with a complex lifestyle such as *C. jejuni* often possess MarR orthologs or
376 paralogs, which regulate genes in response to stress, including degradation of harmful
377 phenolic compounds (2, 30, 42). MarR homologs are usually in genomic loci that are
378 composed of divergently oriented genes encoding the transcriptional regulator and the
379 gene(s) under its control (43). Interestingly, *mdaB* and *nfrA* are located divergently oriented
380 upstream *rrpA* and *rrpB*, respectively. Analysis of DNA substrate interaction assays showed
381 RrpA and RrpB bind sequences with inverted repeats (IRs) upstream of the translation start
382 site of themselves and their target genes on the intergenic regions of the DNA, a common
383 feature of this regulator family (44, 45). The identified protected regions led us to speculate
384 that it is likely that the binding sites for RrpA are close enough to the promoter regions of
385 *mdaB* and *rrpA* for the RNA polymerase to initiate transcription, in contrast, RrpB binding
386 sites are distal from the RNA polymerase binding site, and RrpB repression mechanism is by
387 destabilizing the DNA open complex (43).

388

389 In *C. jejuni*, *mdaB* was reported to have a role in oxidative stress, yet the specific role for its
390 product has been elusive (3, 46, 47). We present evidence to show that both *mdaB* and its
391 regulator RrpA respond to quinones. The redox-active quinone compounds can be
392 competitively reduced to hydroquinone via a two-electron mechanism by NADPH-quinone
393 reductases (33, 38, 48). Semiquinone radicals are cytotoxic due to their ability to react with
394 molecular oxygen and in turn generate superoxide radicals (23). The two-electron transfer
395 pathway of quinones produces quinols, this two-step pathway minimizes cellular damage due
396 to the inability of quinols to cause oxidative stress. In *Escherichia coli*, quinols have been

397 shown to lower the levels of superoxide ions in cell membrane (49). Our results indicate that
398 *C. jejuni* MdaB is a quinone reductase with broad substrate specificity, and treatment of *C.*
399 *jejuni* $\Delta mdaB$ and $\Delta rrpA$ mutants with quinone showed reduction of growth compared to the
400 parental strain. In both the external environment and in the host and the gut, many organisms
401 synthesize toxic quinones (50) and derivatives that form core constituents of many
402 antimicrobial compounds (51-53). It is plausible that *C. jejuni* would come into contact with
403 these compounds. We propose that MdaB contributes to the protection of *C. jejuni* from
404 production of semiquinones by competing with the quinone one-electron reduction pathway,
405 as also suggested by Palyada *et al.* (26).

406

407 The NADPH-flavin reductase described here is the product of *nfrA* gene, it belongs to the
408 family of flavin reductases that were first isolated from luminous marine bacteria (54, 55) and
409 from human erythrocytes (56). Given that it took a high concentration of riboflavin to have an
410 effect on growing *C. jejuni* $\Delta nfrA$ mutant strain and NfrA reduces riboflavin at a much higher
411 rate than its 5' -phosphorylated form (FMN), which is produced by riboflavin kinase within
412 the cell, is suggestive that unidentified exogenous free flavins are its natural substrates. A
413 recent study has identified a chemical analogue of riboflavin that has antimicrobial activity.
414 Roseoflavin (8-demethyl-8-dimethylamino-riboflavin) is a broad-spectrum antibiotic
415 naturally produced by *Streptomyces spp.* and has been shown to be effective against several
416 bacterial species and protozoans (57). Import of this compound was shown to be mediated by
417 riboflavin transporters and cellular targets for roseoflavin included FMN riboswitches and
418 flavoproteins (58, 59). Many bacteria employ FMN riboswitches and all cells depend on the
419 activity of flavoproteins for homeostasis, so inhibition of these systems can be detrimental to
420 the cell. Similarly to other flavins, roseoflavin has the potential to generate highly toxic
421 reactive semiquinones (60). Thus, we speculate that NfrA reduces flavin compounds via the

422 two-electron reductant pathway, protecting *C. jejuni* against reactive flavo-semiquinones and
423 flavin analogues.

424

425 The distribution of *mdaB* and *nfrA* in 374 *Campylobacter* spp. and 253 *Helicobacter* spp.

426 complete genome sequences was studied (**Supplementary Table. S3a and Table. S3b**).

427 *mdaB* was present in all 627 genome sequences analyzed despite the absence of *rrpA*. *nfrA*

428 was absent in *Helicobacter* spp. sequences analyzed, whilst in the majority *Campylobacter*

429 spp., *nfrA* was predicted as incomplete. In the majority of *Campylobacter* spp. sequences that

430 lacked a complete *nfrA*, *rrpB* was either absent or partially present. This suggested that *mdaB*

431 is important in both organisms. Furthermore, *C. jejuni* strains that are less frequently isolated

432 in human infections lack a complete *nfrA*, this is indicative that these strains have an as yet

433 unidentified mechanism of flavin reduction.

434

435 RrpA and RrpB share conserved cysteines (Cys) with other MarR family transcription

436 regulators and *in vitro* post translational modification analysis indicated these Cys residues

437 are modified by oxidizing compounds. Our results showed the importance of the conserved

438 Cys13 in RrpA for dimerization but not for DNA binding. Studies have shown that MarR

439 transcription regulators form homodimers and their transcriptional regulation ability, but not

440 DNA binding ability, can depend on the dimeric form (30, 61). We speculate that RrpA

441 Cys13 is most likely important for transcription regulation. Mutation to the non-conserved

442 RrpA Cys8, led to its inability to bind DNA substrate possibly due to structure

443 destabilization. Further work will be needed to investigate the role of Cys 8 in RrpA

444 structure. Similarly, RrpB_{Cys8Ser} was unable to dimerize or form protein-DNA complex with

445 its substrates, and interestingly treatment with redox cycling compound had the same effects

446 as the mutation to RrpB Cys8. *In vitro* PTM indicated RrpB Cys8 is modified to the

447 irreversible thiosulfonic acid, we propose that the de-repression mechanism of RrpB is due to
448 oxidation modification to Cys8. In *E. coli*, the SoxRS regulatory system detects and is
449 oxidized by redox cycling compounds such as quinones, and one of the members of the
450 SoxRS regulon is *mdaB* (62). From our work, it is now apparent that although *C. jejuni* has
451 long been known to lack *soxRS* genes, the RrpA and RrpB system described here is at least
452 partly functional analogous. A model for how we believe the regulatory proteins and
453 protective enzymes allow *C. jejuni* to combat quinone and flavin mediated oxidative stress is
454 shown in **Fig. 8**.

455

456 We also noted other genes were differentially regulated in our regulator mutants, and
457 although the expression levels were not necessarily related to functional importance, it is
458 possible that mutations in *rrpA* and *rrpB* may affect other pathways that are not investigated
459 here, in particular, ribosomal genes, autotransporters and amino acid metabolism. However, it
460 is interesting that expression of *leuA* was increased in the *rrpAB* double mutant. The
461 dehydratase enzymes (LeuCD) of the branched chain amino-acid biosynthesis pathway
462 contain labile Fe-S clusters and have long been known to be targets for ROS damage in *E.*
463 *coli* (63) and perhaps *leuA* upregulation reflects this.

464

465 **Conclusion**

466 MdaB and NfrA are reductases specific to their substrates and are under the control of the
467 redox regulators RrpA and RrpB, respectively. MdaB catalyzes the reduction of quinones,
468 whilst NfrA is a flavin reductase, thus it is possible that both enzymes contribute to *C. jejuni*
469 protection against potential reactive semiquinone species. We propose that possession of
470 these enzymes by *C. jejuni* is important during its *in vivo* and *ex vivo* life-cycle and could be
471 a significant factor for the persistence and prevalence of *C. jejuni* in the food chain.

472

473 **Methods**474 **Bacterial cultures and strains**

475 Bacteria were stored using Protect bacterial preservers (Technical Service Consultants,
476 Heywood, U.K.) at -80°C . *C. jejuni* strains, were streaked on blood agar (BA) plates
477 containing Columbia agar base (Oxoid) supplemented with 7% (v/v) horse blood (TCS
478 Microbiology, UK) and Campylobacter Selective Supplement (Oxoid), and grown at 37°C in
479 a microaerobic chamber (Don Whitley Scientific, UK), containing 85% N_2 , 10% CO_2 , and
480 5% O_2 for 48 hrs. *C. jejuni* strains were grown on Columbia blood agar (CBA) plates for a
481 further 16 hrs prior to use. Strain 11168H of Multilocus Sequence Type (MLST) clonal
482 complex ST-21, a hypermotile derivative of the original strain NCTC11168 that shows a
483 higher level of caeca colonization in a chick model (8) was used in this study. Construction of
484 mutants in which *rrpA* and *rrpB* have been inactivated to give isogenic mutants $\Delta rrpA$ and
485 $\Delta rrpB$ has been previously described (6, 7).

486

487 **Protein expression and purification**

488 Recombinant RrpA, RrpB and their variants RrpA_{Cys8Ser}, RrpA_{Cys13Ser}, RrpA_{Cys33Ser},
489 RrpA_{Cys113Ser}, RrpB_{Cys8Ser} and MdaB and NfrA were cloned into pET21a⁺ plasmid using
490 NEBuilder® HiFi DNA Assembly Cloning Kit (New England Biolabs). The proteins were
491 overexpressed in *E. coli* strain BL21(DE3). The cells were grown in LB broth containing
492 0.6% Glycerol, 0.05% glucose and 0.2% lactose and 100 $\mu\text{g}/\text{mL}$ Ampicillin at 37°C
493 overnight. Cells were harvested by centrifugation at $4,000 \times g$ for 15 mins at 4°C and
494 resuspended in buffer A (20 mM Tris-HCl, pH 8.0 500 mM NaCl, 5% (vol/vol) glycerol, 5
495 mM 2-Mercaptoethanol containing EDTA-free Complete Protease Inhibitor Mixture (Roche))
496 for lysis. Cell debris were removed by centrifugation at $10,000 \times g$ for 30 min at 4°C . The

497 supernatant was incubated with Ni-NTA agarose nickel-charged resins (Qiagen) that had
498 been equilibrated in buffer A. The protein bound resin was washed with buffer A containing
499 15 mM imidazole and eluted with buffer A containing 400 mM imidazole. Primers used to
500 generate recombinant proteins are presented in Supplementary file 4 (**Table. S4a**).

501

502 **Gene expression by RNA-Seq and bioinformatics analysis**

503 RNA-Seq was used to identify differentially expressed genes between wild type strains,
504 $\Delta rrpA$ and $\Delta rrpB$ mutants at mid-log (~6 hrs) of growth. *C. jejuni* 11168H wild type,
505 11168H $\Delta rrpA$, 11168H $\Delta rrpB$ and 11168H $\Delta rrpAB$ were plated out on BA plates and
506 incubated at 37 °C under microaerobic conditions for 6 hrs, 25 ml of pre-incubated brucella
507 was inoculated with *C. jejuni* strains at an OD_{600nm} 0.1 and grown at 37 °C under
508 microaerobic conditions as described above. Transcription was stopped by RNA protect
509 (Qiagen), RNA was extracted by PureLink™ RNA Mini Kit (Invitrogen), following
510 manufactures protocol. Ribosomal RNA was depleted using Ribominus (Invitrogen) and
511 libraries was prepared using TruSeq® Stranded mRNA (Illumina). Raw reads were obtained
512 from an Illumina MiSeq paired-end sequencing platform (Illumina). The paired-end reads
513 were trimmed and filtered using Sickle v1.200 (64), Bowtie2 (65) was used to map the reads
514 against the reference sequence; *C. jejuni* strains 11168H assembly GCA_900117385.1.
515 Cufflinks suite (66) was used to convert annotations from GFF to GTF format and Bedtools
516 (67) was used to generate transcript counts per samples. Statistical analysis was performed in
517 R using the combined data generated from the bioinformatics as well as meta data associated
518 with the study (multifactorial design). Adjusted *p*-value significance cut-off of 0.05 and log
519 fold change cut-off of >1.5 was used for multiple comparison.

520

521 **Real-time RT-qPCR**

522 Expression of genes of interest were quantified by real-time RT-qPCR and normalized
523 against *gyrA*. A 1 µg volume of total RNA of each sample was reverse-transcribed to cDNA
524 using RT² first strand kit (Qiagen) according to manufactures protocol. Quantification of
525 gene expression was achieved by real-time RT-qPCR using TaqMan primers and probes
526 created by the Assay-by-Design Service of Applied Biosystems (**Table. S4b**). Real-time RT-
527 PCR was performed in 96-well plates using an ABI PRISM 7300 Real-time PCR System
528 (Applied Biosystems) and the relative gene expression for the different genes was calculated
529 from the crossing threshold (Ct) value according to the manufacturer's protocol ($2^{-\Delta\Delta Ct}$) after
530 normalization using the *gyrA* endogenous control (68).

531

532 **DNase I footprinting and electrophoretic mobility shift assay**

533 DNase I footprinting was performed as previously described (29). Briefly, a 393 bp DNA
534 fragment was PCR amplified with primers modified with Fluorescein amidite (FAM) and
535 Hexachloro-fluorescein (HEX). Primers were used to amplify regions upstream of the
536 translation initiation sites of *rrpA* and *mdaB* (cj1546Ffam and cj1546Rhex), and for *rrpB* and
537 *nfrA* (cj1556Ffam and cj1556Rhex). PCR was performed for 30 cycles at the following
538 conditions: 95 °C for 60 sec, 58 °C for 60 sec, 72 °C for 60 sec. The FAM/HEX-labelled
539 probes were cleaned using QiAquick PCR purification kit (Qiagen) and quantified with
540 NanodropTM spectrometer (Thermo Scientific). For the DNase I footprinting assay, 500 ng
541 probes were incubated with varying concentration (from 20 µg to 0 µg) of RrpA_{his6} or
542 RrpB_{his6} in a total volume of 40 µl in buffer containing (30 mM potassium glutamate, 1 mM
543 dithiothreitol (DTT), 5 mM magnesium acetate, 2 mM CaCl₂, 0.125 mg/mL bovine serum
544 albumin (BSA), 30% glycerol in 10 mM Tris HCl, pH 8.5). After incubation for 20 min at 25
545 °C, 10 µl of 0.02 unit of DNase I (NEB) was added to the binding reaction and incubated for
546 a further 5 mins at 25 °C. The DNase I was inactivated by incubating the reaction at 74 °C

547 for 10 mins. Samples were cleaned and eluted in 20 μ l of dH₂O. The samples were run with
548 the 3730 DNA Analyzer and viewed with Gene mapper v6 (Applied Biosystems).

549

550 For EMSA, purified RrpA_{his6} (0.05 μ g) was incubated with IRDye® 800 DNA fragments
551 spanning the identified binding regions upstream of the translation start sites of *mdaB*
552 (*mdaB*probe) and *rrpA* (*rrpA*probe) and RrpB_{his6} (0.05 μ g) with *nfrA* (*nfrA*probe) and *rrpB*
553 (*rrpB*probe), a 50 nm probe was used in a 20 μ l reaction. Odyssey® Infrared EMSA kit (LI-
554 COR Biosciences) was used according to the manufacture instructions. Samples were loaded
555 in a pre-cast 6% Novex® DNA retardation gel (Life Technologies) and run at 4 °C and gels
556 were analyzed on a LI-COR Odyssey® imaging scanner (LI-COR Biosciences). List of
557 primers for DNase I footprinting and probes for EMSA are found in **Table. S4c**.

558

559 ***In vitro* post translation modification analysis using LC-MS/MS**

560 Recombinant (1 μ g) RrpA_{his6} was treated with 50 μ M 2-hydroxy-1,4-napthoquinone or 50
561 μ M H₂O₂ and RrpB_{his6} was treated with 100 μ M H₂O₂ for 30 mins at room temperature.
562 Samples were resuspended in 500 μ l of 50 mM tetraethylammonium bicarbonate (TEAB;
563 Sigma), vortexed, and centrifuged at 14,000 rpm for 1 min. Overnight trypsin digestion at 37
564 °C was performed without the reduction and alkylation of cysteine residues to protect post-
565 translational modification. Samples were dried and resuspended in 40 μ l of 2% acetonitrile in
566 0.05% formic acid, 10 μ l of which was injected to be analyzed by LC-MS/MS.

567 Chromatographic separation was performed using a U3000 UHPLC NanoLC system
568 (Thermo Fisher Scientific). Peptides were resolved by reversed phase chromatography on a
569 75 μ m C18 Pepmap column (50 cm length) using a four-step linear gradient of 80%
570 acetonitrile in 0.1% formic acid. Raw mass spectrometry data was processed into peak list
571 files using Proteome Discoverer (Thermo Fischer Scientific; v2.2). The raw data file was

572 processed and searched using the Sequest search algorithm (69) against a bespoke database
573 containing the RrpA and RrpB protein sequences obtained from Uniprot ([Q0P879](#) (RrpA) and
574 [Q0P870](#) (RrpB)).

575

576 **Reductase assays**

577 An assay mixture consisting of 50 mM Tris-HCl, 100 mM NaCl, 10 % v/v DMSO, 200 μ M
578 NADPH and 2 μ M MdaB was sparged with oxygen-free nitrogen for 7 mins, followed by
579 incubation at 37 °C for 2 mins. Absorbance was recorded at 360 nm for 30 secs before the
580 addition of 0.2 mM substrate. NADPH consumption was recorded for a further 1.5 mins.
581 FMN and FAD were prepared in dH₂O, while riboflavin was prepared in 10 mM NaOH,
582 NfrA activity was determined at an absorbance of 340 nm and NAD(P)H consumption was
583 recorded for a further 3 mins. No protein controls were performed with all substrates.

584

585 **Growth measurement**

586 Brucella broth was pre-incubated at 37 °C under microaerobic conditions for 24 hrs.
587 Following overnight growth on BA, the bacteria cells were sub-cultured in 10 ml of the pre-
588 incubated broth in a 30 ml flask at an OD_{600nm} = 0.01 at 37 °C under microaerobic conditions
589 and grown to OD_{600nm} = 0.4. Compounds were added to the respective strains at a
590 concentration indicated and OD_{600nm} readings were performed at selected time points.

591

592 **Statistics**

593 Statistical analysis for RNA-Seq were performed in R using the combined data generated
594 from the bioinformatics as well as meta data associated with the study (multifactorial design).
595 Differentially expressed genes were considered significant when the *p*-value of five
596 independent biological experiments was below 0.05. For other experiments two-way

597 ANOVA with Šídák multiple comparison test and student t-tests were performed to obtain *p*-
598 values using the software GraphPad Prism (Version 9, GraphPad Software, Inc.).

599

600 **Data availability:** The data that support the RNA-seq findings of this study are openly
601 available in Gene Expression Omnibus (GEO) at <https://www.ncbi.nlm.nih.gov/geo/>, dataset
602 identifier: GSE174333. Data that supports the post translational modification finding of this
603 study are openly available in ProteomeXchange via the PRIDE database at
604 <http://doi.org/10.6019/PXD025924>, dataset identifier: PXD025924.

605

606 **Acknowledgments:** We thank Nick Dorrell for his advice. We also thank Cadi Davies for
607 sharing her protocol on RNA-Seq and Teresa Cortes for her guidance to RNA-Seq analysis.

608

609 **Author contributions:** F.N., conceptualized the study; F.N., A.E., A.T., D.B., R.G., and B.L.
610 performed the research; A.E., D.B., O.G., R.G., U. Z. I., and S.L., contributed analytic tools;
611 F.N., A.E., A.T., D.B., U.Z. I., D.S., B.L., S.L., and D.J.K., analyzed the data. F.N., A.T.,
612 S.L., B.L., D.J.K and B.W., wrote the manuscript. All authors reviewed the manuscript.

613

614 **Funding:** This work was supported by Biotechnology and Biological Sciences Research
615 Council Institute Strategic Program BB/R012504/1 constituent project BBS/E/F/000PR10349
616 to B.W. A.J.T was supported by BBSRC grant BB/S014497/1 to D.J.K. U.Z.I. is supported
617 by NERC IRF NE/L011956/1. The funders had no role in study design, data collection and
618 interpretation, or the decision to submit the work for publication.

619

620 **Conflict of Interest Statement:** The authors declare that the research was conducted in the
621 absence of any commercial or financial relationships that could be construed as a potential
622 conflict of interest.

623

624 **References**

- 625 1. Igwaran A, Okoh AI. 2019. Human campylobacteriosis: A public health concern of global
626 importance. *Heliyon* 5:e02814-e02814.
- 627 2. Brenner D, Krieg N, Staley J, Garrity G. 2005. *Bergey's Manual of Systematic Bacteriology*,
628 2nd edn, vol. 2B. New York: Springer.
- 629 3. Flint A, Stintzi A, Saraiva LM. 2016. Oxidative and nitrosative stress defences of *Helicobacter*
630 and *Campylobacter* species that counteract mammalian immunity. *FEMS microbiology*
631 *reviews* 40:938-960.
- 632 4. Atack JM, Harvey P, Jones MA, Kelly DJ. 2008. The *Campylobacter jejuni* thiol peroxidases
633 Tpx and Bcp both contribute to aerotolerance and peroxide-mediated stress resistance but
634 have distinct substrate specificities. *Journal of bacteriology* 190:5279-5290.
- 635 5. Baillon M-LA, Van Vliet AH, Ketley JM, Constantinidou C, Penn CW. 1999. An iron-regulated
636 alkyl hydroperoxide reductase (AhpC) confers aerotolerance and oxidative stress resistance
637 to the microaerophilic pathogen *Campylobacter jejuni*. *Journal of Bacteriology* 181:4798-
638 4804.
- 639 6. Gundogdu O, Mills DC, Elmi A, Martin MJ, Wren BW, Dorrell N. 2011. The *Campylobacter*
640 *jejuni* transcriptional regulator Cj1556 plays a role in the oxidative and aerobic stress
641 response and is important for bacterial survival in vivo. *Journal of bacteriology* 193:4238-
642 4249.
- 643 7. Gundogdu O, da Silva DT, Mohammad B, Elmi A, Mills DC, Wren BW, Dorrell N. 2015. The
644 *Campylobacter jejuni* MarR-like transcriptional regulators RrpA and RrpB both influence
645 bacterial responses to oxidative and aerobic stresses. *Frontiers in microbiology* 6:724-724.
- 646 8. Jones MA, Marston KL, Woodall CA, Maskell DJ, Linton D, Karlyshev AV, Dorrell N, Wren BW,
647 Barrow PA. 2004. Adaptation of *Campylobacter jejuni* NCTC11168 to high-level colonization
648 of the avian gastrointestinal tract. *Infection and immunity* 72:3769-3776.
- 649 9. Karlyshev AV, Linton D, Gregson NA, Wren BW. 2002. A novel paralogous gene family
650 involved in phase-variable flagella-mediated motility in *Campylobacter jejuni*. *Microbiology*
651 148:473-480.
- 652 10. Gundogdu O, da Silva DT, Mohammad B, Elmi A, Wren BW, van Vliet AHM, Dorrell N. 2016.
653 The *Campylobacter jejuni* Oxidative Stress Regulator RrpB Is Associated with a Genomic
654 Hypervariable Region and Altered Oxidative Stress Resistance. *Frontiers in microbiology*
655 7:2117-2117.
- 656 11. Newman DJ, Cragg GM. 2016. Natural products as sources of new drugs from 1981 to 2014.
657 *Journal of natural products* 79:629-661.
- 658 12. Kurosu M, Begari E. 2010. Vitamin K2 in Electron Transport System: Are Enzymes Involved in
659 Vitamin K2 Biosynthesis Promising Drug Targets? *Molecules* 15:1531-1553.
- 660 13. Kumagai Y, Koide S, Taguchi K, Endo A, Nakai Y, Yoshikawa T, Shimojo N. 2002. Oxidation of
661 proximal protein sulfhydryls by phenanthraquinone, a component of diesel exhaust
662 particles. *Chemical research in toxicology* 15:483-489.

- 663 14. McDonald T, Holland N, Skibola C, Duramad P, Smith M. 2001. Hypothesis: phenol and
664 hydroquinone derived mainly from diet and gastrointestinal flora activity are causal factors
665 in leukemia. *Leukemia* 15:10-20.
- 666 15. Monks TJ, Hanzlik RP, Cohen GM, Ross D, Graham DG. 1992. Quinone chemistry and toxicity.
667 *Toxicology and applied pharmacology* 112:2-16.
- 668 16. O'Brien P. 1991. Molecular mechanisms of quinone cytotoxicity. *Chemico-biological*
669 *interactions* 80:1-41.
- 670 17. Armstrong W, Spink WW, Kahnke J. 1943. Antibacterial Effects of Quinones. *Proceedings of*
671 *the Society for Experimental Biology and Medicine* 53:230-234.
- 672 18. Cohen GM, d'Arcy Doherty M. 1987. Free radical mediated cell toxicity by redox cycling
673 chemicals. *Br J Cancer Suppl* 8:46-52.
- 674 19. Mansoorabadi SO, Thibodeaux CJ, Liu H-w. 2007. The diverse roles of flavin coenzymes--
675 nature's most versatile thespians. *The Journal of organic chemistry* 72:6329-6342.
- 676 20. Kao Y-T, Saxena C, He T-F, Guo L, Wang L, Sancar A, Zhong D. 2008. Ultrafast dynamics of
677 flavins in five redox states. *Journal of the American Chemical Society* 130:13132-13139.
- 678 21. Di Francesco AM, Ward TH, Butler J. 2004. Diaziridinylbenzoquinones. *Methods in*
679 *enzymology* 382:174-193.
- 680 22. Tomonori Suzuki AA, Shinji Kawasaki, Masataka Uchino, Etsuo Yoshimura, Akio Watanabe,
681 Ken Kitano, Daichi Mochizuki, Kouji Takeda, Junichi Satoh, Shinya Kimata and Youichi
682 Niimura. 2020. Free Flavins Participates in Iron and Also Oxygen Metabolism in Bacteria.
683 *Journal of Bacteriology & Parasitology* 11.
- 684 23. Bolton JL, Trush MA, Penning TM, Dryhurst G, Monks TJ. 2000. Role of quinones in
685 toxicology. *Chem Res Toxicol* 13:135-60.
- 686 24. Chaiyen P, Fraaije MW, Mattevi A. 2012. The enigmatic reaction of flavins with oxygen.
687 *Trends Biochem Sci* 37:373-80.
- 688 25. Hong Y, Wang G, Maier RJ. 2008. The NADPH quinone reductase MdaB confers oxidative
689 stress resistance to *Helicobacter hepaticus*. *Microbial pathogenesis* 44:169-174.
- 690 26. Palyada K, Sun Y-Q, Flint A, Butcher J, Naikare H, Stintzi A. 2009. Characterization of the
691 oxidative stress stimulon and PerR regulon of *Campylobacter jejuni*. *BMC genomics* 10:481.
- 692 27. Kyuma T, Kizaki H, Ryuno H, Sekimizu K, Kaito C. 2015. 16S rRNA methyltransferase KsgA
693 contributes to oxidative stress resistance and virulence in *Staphylococcus aureus*. *Biochimie*
694 119:166-174.
- 695 28. Zhang-Akiyama Q-M, Morinaga H, Kikuchi M, Yonekura S-I, Sugiyama H, Yamamoto K, Yonei
696 S. 2009. KsgA, a 16S rRNA adenine methyltransferase, has a novel DNA glycosylase/AP lyase
697 activity to prevent mutations in *Escherichia coli*. *Nucleic acids research* 37:2116-2125.
- 698 29. Sivapragasam S, Pande A, Grove A. 2015. A recommended workflow for DNase I footprinting
699 using a capillary electrophoresis genetic analyzer. *Analytical Biochemistry* 481:1-3.
- 700 30. Grove A. 2013. MarR family transcription factors. *Current biology* 23:R142-R143.
- 701 31. Ryan A, Kaplan E, Nebel JC, Polycarpou E, Crescente V, Lowe E, Preston GM, Sim E. 2014.
702 Identification of NAD(P)H quinone oxidoreductase activity in azoreductases from *P.*
703 *aeruginosa*: azoreductases and NAD(P)H quinone oxidoreductases belong to the same FMN-
704 dependent superfamily of enzymes. *PLoS One* 9:e98551.
- 705 32. Hayashi M, Ohzeki H, Shimada H, Unemoto T. 1996. NADPH-specific quinone reductase is
706 induced by 2-methylene-4-butyrolactone in *Escherichia coli*. *Biochim Biophys Acta* 1273:165-
707 70.
- 708 33. Wang G, Maier RJ. 2004. An NADPH quinone reductase of *Helicobacter pylori* plays an
709 important role in oxidative stress resistance and host colonization. *Infection and immunity*
710 72:1391-1396.
- 711 34. Bardwell JC. 2004. The dance of disulfide formation. *Nature structural & molecular biology*
712 11:582-583.

- 713 35. Kim HJ, Ha S, Lee HY, Lee KJ. 2015. ROSics: chemistry and proteomics of cysteine
714 modifications in redox biology. *Mass spectrometry reviews* 34:184-208.
- 715 36. Madeira F, Park YM, Lee J, Buso N, Gur T, Madhusoodanan N, Basutkar P, Tivey ARN, Potter
716 SC, Finn RD, Lopez R. 2019. The EMBL-EBI search and sequence analysis tools APIs in 2019.
717 *Nucleic acids research* 47:W636-W641.
- 718 37. Champion OL, Gaunt MW, Gundogdu O, Elmi A, Witney AA, Hinds J, Dorrell N, Wren BW.
719 2005. Comparative phylogenomics of the food-borne pathogen *Campylobacter jejuni* reveals
720 genetic markers predictive of infection source. *Proceedings of the National Academy of
721 Sciences of the United States of America* 102:16043.
- 722 38. Adams MA, Jia Z. 2006. Modulator of drug activity B from *Escherichia coli*: crystal structure
723 of a prokaryotic homologue of DT-diaphorase. *J Mol Biol* 359:455-65.
- 724 39. Adams MA, Iannuzzi P, Jia Z. 2005. MdaB from *Escherichia coli*: cloning, purification,
725 crystallization and preliminary X-ray analysis. *Acta crystallographica Section F, Structural
726 biology and crystallization communications* 61:235-238.
- 727 40. Wang Z, Li L, Dong YH, Su XD. 2014. Structural and biochemical characterization of MdaB
728 from cariogenic *Streptococcus mutans* reveals an NADPH-specific quinone oxidoreductase.
729 *Acta Crystallogr D Biol Crystallogr* 70:912-21.
- 730 41. Sepúlveda Cisternas I, Salazar JC, García-Angulo VA. 2018. Overview on the Bacterial Iron-
731 Riboflavin Metabolic Axis. *Frontiers in microbiology* 9:1478-1478.
- 732 42. Loi VV, Busche T, Tedin K, Bernhardt J, Wollenhaupt J, Huyen NTT, Weise C, Kalinowski J,
733 Wahl MC, Fulde M. 2018. Redox-sensing under hypochlorite stress and infection conditions
734 by the Rrf2-family repressor HypR in *Staphylococcus aureus*. *Antioxidants & redox signaling*
735 29:615-636.
- 736 43. Deochand DK, Grove A. 2017. MarR family transcription factors: dynamic variations on a
737 common scaffold. *Critical reviews in biochemistry and molecular biology* 52:595-613.
- 738 44. Otani H, Stogios PJ, Xu X, Nocek B, Li S-N, Savchenko A, Eltis LD. 2015. The activity of CouR, a
739 MarR family transcriptional regulator, is modulated through a novel molecular mechanism.
740 *Nucleic Acids Research* 44:595-607.
- 741 45. Fiorentino G, Ronca R, Cannio R, Rossi M, Bartolucci S. 2007. MarR-Like Transcriptional
742 Regulator Involved in Detoxification of Aromatic Compounds in *Sulfolobus*
743 *solfataricus*. *Journal of Bacteriology* 189:7351.
- 744 46. Guccione E, Kendall J, Hitchcock A, Garg N, White M, Mulholland F, Poole R, Kelly D. 2017.
745 Transcriptome and proteome dynamics in chemostat culture reveal how *Campylobacter*
746 *jejuni* modulates metabolism, stress responses and virulence factors upon changes in oxygen
747 availability: Global oxygen responses of *C. jejuni*. *Environmental Microbiology* 19.
- 748 47. Flint A, Sun Y-Q, Butcher J, Stahl M, Huang H, Stintzi A. 2014. Phenotypic screening of a
749 targeted mutant library reveals *Campylobacter jejuni* defenses against oxidative stress.
750 *Infection and immunity* 82:2266-2275.
- 751 48. Adams MA, Jia Z. 2005. Structural and biochemical evidence for an enzymatic quinone redox
752 cycle in *Escherichia coli*: identification of a novel quinol monooxygenase. *J Biol Chem*
753 280:8358-63.
- 754 49. Søballe B, Poole RK. 2000. Ubiquinone limits oxidative stress in *Escherichia coli*. *Microbiology*
755 146:787-796.
- 756 50. Babula P, Adam V, Havel L, Kizek R. 2009. Noteworthy secondary metabolites
757 naphthoquinones-their occurrence, pharmacological properties and analysis. *Current
758 Pharmaceutical Analysis* 5:47-68.
- 759 51. Atkinson DJ, Brimble MA. 2015. Isolation, biological activity, biosynthesis and synthetic
760 studies towards the rubromycin family of natural products. *Natural product reports* 32:811-
761 840.
- 762 52. Carcamo-Noriega EN, Sathyamoorthi S, Banerjee S, Gnanamani E, Mendoza-Trujillo M, Mata-
763 Espinosa D, Hernández-Pando R, Veytia-Bucheli JI, Possani LD, Zare RN. 2019. 1,4-

- 764 Benzoquinone antimicrobial agents against *Staphylococcus aureus* and
765 *Mycobacterium tuberculosis* derived from scorpion venom. Proceedings of the
766 National Academy of Sciences 116:12642.
- 767 53. Oka S. 1962. Mechanism of Antimicrobial Effect of Quinone Compounds: Part III. Inactivation
768 of p-Benzoquinone by its Addition Reaction with Amino Compounds in Culture MediumPart
769 IV. Germicidal Effect and Growth Inhibiting Effect. Agricultural and Biological Chemistry
770 26:500-514.
- 771 54. GERLO E, CHARLIER J. 1975. Identification of NADH-specific and NADPH-specific FMN
772 reductases in *Beneckea harveyi*. European journal of biochemistry 57:461-467.
- 773 55. Jablonski E, DeLuca M. 1977. Purification and properties of the NADH and NADPH specific
774 FMN oxidoreductases from *Beneckea harveyi*. Biochemistry 16:2932-2936.
- 775 56. Yubisui T, Takeshita M. 1980. Characterization of the purified NADH-cytochrome b5
776 reductase of human erythrocytes as a FAD-containing enzyme. Journal of Biological
777 Chemistry 255:2454-2456.
- 778 57. Mora-Lugo R, Stegmüller J, Mack M. 2019. Metabolic engineering of roseoflavin-
779 overproducing microorganisms. Microbial Cell Factories 18:146.
- 780 58. Langer S, Hashimoto M, Hobl B, Mathes T, Mack M. 2013. Flavoproteins are potential targets
781 for the antibiotic roseoflavin in *Escherichia coli*. Journal of bacteriology 195:4037-4045.
- 782 59. Wang H, Mann PA, Xiao L, Gill C, Galgoci AM, Howe JA, Villafania A, Barbieri CM, Malinverni
783 JC, Sher X. 2017. Dual-targeting small-molecule inhibitors of the *Staphylococcus aureus* FMN
784 riboswitch disrupt riboflavin homeostasis in an infectious setting. Cell chemical biology
785 24:576-588. e6.
- 786 60. Muller F. 2019. Chemistry and Biochemistry of Flavoenzymes: Volume III. CRC Press.
- 787 61. Hillion M, Antelmann H. 2015. Thiol-based redox switches in prokaryotes. Biological
788 chemistry 396:415-444.
- 789 62. Gu M, Imlay JA. 2011. The SoxRS response of *Escherichia coli* is directly activated by redox-
790 cycling drugs rather than by superoxide. Molecular microbiology 79:1136-1150.
- 791 63. Jang S, Imlay JA. 2007. Micromolar intracellular hydrogen peroxide disrupts metabolism by
792 damaging iron-sulfur enzymes. Journal of Biological Chemistry 282:929-937.
- 793 64. Joshi N, Fass J. 2011. Sickle: A sliding-window, adaptive, quality-based trimming tool for
794 FastQ files (Version 1.33)[Software].
- 795 65. Langmead B, Salzberg SL. 2012. Fast gapped-read alignment with Bowtie 2. Nature methods
796 9:357.
- 797 66. Trapnell C, Williams BA, Pertea G, Mortazavi A, Kwan G, Van Baren MJ, Salzberg SL, Wold BJ,
798 Pachter L. 2010. Transcript assembly and quantification by RNA-Seq reveals unannotated
799 transcripts and isoform switching during cell differentiation. Nature biotechnology 28:511.
- 800 67. Quinlan AR, Hall IM. 2010. BEDTools: a flexible suite of utilities for comparing genomic
801 features. Bioinformatics 26:841-842.
- 802 68. Ritz M, Garenaux A, Berge M, Federighi M. 2009. Determination of *rpoA* as the most suitable
803 internal control to study stress response in *C. jejuni* by RT-qPCR and application to oxidative
804 stress. J Microbiol Methods 76:196-200.
- 805 69. Eng JK, McCormack AL, Yates JR. 1994. An approach to correlate tandem mass spectral data
806 of peptides with amino acid sequences in a protein database. J Am Soc Mass Spectrom
807 5:976-89.
- 808 70. Wösten MM, Boeve M, Koot MG, van Nuenen AC, van der Zeijst BA. 1998. Identification of
809 *Campylobacter jejuni* promoter sequences. Journal of bacteriology 180:594-599.
- 810
- 811
- 812

813 **Figure Legends:**

814 **Figure. 1. Relative gene expression of a) *mdaB*; b) *nfrA*; c) *capA*; and d) *rsmA*.**

815 Expression of the genes were determined by real-time RT-PCR and are displayed relative to
816 the wild type expression, after normalization with *gyrA*. Data presented is the mean value of
817 at least 3 independent experiments performed on different days, error bars indicate S.D. * $p \leq$
818 0.05; paired Student t-test was used; ** $p \leq 0.01$, *** $p \leq 0.001$.

819

820 **Figure. 2. Electropherograms of fluorescent dye-labelled DNA fragments.** Reduced

821 electropherograms signals indicate protection regions by RrpA_{his6} upstream of **a) *mdaB*** and
822 **b) *rrpA***. Protection regions by RrpB_{his6} upstream of **c) *rrpB***. (Region within the lines indicate
823 protected regions, blue and green electropherograms indicate FAM and Hex fluorescently
824 labelled DNA fragments, respectively. The electropherograms are presented as arbitrary
825 scale). Panels **d** and **e**) show the protected regions by RrpA_{his6} (grey highlight) including the
826 inverted repeat sequence (bold and underlined), upstream of *rrpA* and *mdaB* transcription
827 start sites, panel **f**) shows the protected region by RrpB_{his6} (grey highlight) upstream *rrpB*
828 (inverted repeat sequences are bold and underlined) and panel **g**) sequence alignment of *rrpB*
829 protected region and the region upstream *nfrA* are matched (red asterisks). Nucleotides
830 highlighted in green indicate *C. jejuni* ribosomal binding site (70) and yellow highlight
831 indicates gene translation start site. Electropherograms are representative of three
832 experiments.

833

834 **Figure. 3. Electrophoretic Mobility Shift Assay.** EMSA was conducted to confirm RrpA_{his6}

835 and RrpB_{his6} DNA binding activity; RrpA_{his6} (0.05 μ g) binds upstream **a) *mdaB*** and RrpB_{his6}
836 (0.05 μ g) binds upstream **b) *nfrA***. RrpA_{his6} binds upstream **c) *rrpA***; and RrpB_{his6} binds
837 upstream **d) *rrpB***; Binding is indicated by shift of band (red arrows). IRDye® 800 DNA
838 fragments were used and imaged with LICOR.

839

840 **Figure 4. *mdaB* and *nfrA* respond to structurally diverse quinones and flavins.**

841 Expression levels of **a)** *mdaB* and *rrpA*; **b)** *mdaB* in Δ *rrpA* mutant strain at 15 mins after
842 treatment with 100 μ M of quinones; and **c)** *nfrA* and *rrpB* at 15 mins after treatment with 100
843 μ M of flavins. Growth in brucella broth was determined by measuring OD_{600nm} every 15
844 mins after addition of **d)** 100 μ M 2-hydroxy-1,4-naphthoquinone to 11168H, Δ *rrpA* and
845 Δ *mdaB* strains and **e)** 500 μ M riboflavin to 11168H, Δ *rrpB* and Δ *nfrA* strains at OD_{600nm} =
846 ~0.45. Cell viability was determined at 60 mins and 120 mins after treatment with **f)** 100 μ M
847 of 2-hydroxy-1,4-naphthoquinone and **g)** 500 μ M of Riboflavin. Gene expression was
848 determined by real-time RT-qPCR after treatment with compounds and is displayed relative
849 to the value of the control expression, after normalization with *gyrA* expression. The values
850 are the means of at least three independent experiments. Error bars = SD., * $p \leq 0.05$,
851 ** $p \leq 0.01$, *** $p \leq 0.001$.

852

853 **Figure 5. Reductase activity of purified recombinant MdaB and NfrA.** **a)** UV–visible
854 spectrum of MdaB showing characteristic flavin cofactor absorbance peaks, inset shows the
855 magnified view of the absorption spectra; **b)** Traces of quinone reductase assay with purified
856 MdaB_{his6} and NADPH (average of triplicates); **c)** Specific activity of MdaB_{his6} with quinone
857 substrates calculated from initial rate (arrow indicate <0); **d)** Riboflavin reductase activity of
858 purified NrfA_{his6} showing preference for NADPH over NADH; **e)** Specific activity of
859 NrfA_{his6} with flavin substrates and NADPH; **f)** Direct measurement of riboflavin reduction by
860 NrfA_{his6} and NADPH anaerobically by following the riboflavin absorbance maximum of 445
861 nm. All assays were performed at pH ~7.5.

862

863 **Figure 6. The effect of redox cycling compounds on protein-DNA complex.** EMSA was
864 used to test the effect of 10 μM 2-hydroxy-1,4-naphthoquinone and 50 μM H_2O_2 on 0.05 μg
865 of RrpA_{his6} binding to its DNA substrates **a)** *mdaB* and **b)** *rrpA*; and the effect of H_2O_2 on
866 0.05 μg of RrpB_{his6} binding to its substrates **c)** *nfrA* and **d)** *rrpB*. Binding is indicated by shift
867 of band (red arrows). IRDye® 800 DNA fragments were used.

868

869 **Figure 7. Identification of conserved cysteine residues in RrpA and RrpB proteins.** a)
870 Sequence alignment of RrpA and RrpB with other MarR family transcriptional regulators; **b)**
871 RrpA_{his6}, RrpB_{his6} and their variants were subjected to non-reducing SDS-PAGE analysis;
872 **c)** RrpA and RrpB variants with mutation to cysteine residues were generated and EMSAs
873 were conducted to determine their role DNA substrate binding; **e)** RrpA_{cys8Ser}, RrpA_{cys13Ser},
874 RrpA_{cys33Ser}, RrpA_{cys113Ser} and **f)** RrpB_{cys8Ser}. Approximately 0.05 ng of RrpA and 0.05 ng of
875 RrpB variants in the presence of 50 nM DNA substrate was used (the red arrows indicate
876 protein-DNA substrate complexes). Clustal Omega was used for multiple sequence
877 alignment, yellow highlight with red asterisk indicate conserved Cys across all MarR family
878 transcription regulators, grey highlight indicates non-conserved Cys in RrpA.

879

880 **Figure 8. Model for the activation of expression and function of MdaB and NfrA by**
881 **RrpA and RrpB.** Structurally diverse quinones (Q) and flavins (F) produced by other
882 bacteria in the intestinal microbiota or other environments encountered by *C. jejuni* enter the
883 cell where they easily abstract single electrons from the flavins or metal centers of cellular
884 redox enzymes (62) to form partially reduced semiquinones (SQ) or flavo-semiquinones
885 (FSQ). In the presence of molecular oxygen, these can lead to the formation of toxic
886 superoxide and other ROS (hydrogen peroxide), which may be dealt with by superoxide
887 dismutase, catalase and thiol peroxidases (AhpC, Tpx and Bcp). Elevated ROS leads to

888 oxidation of Cys13 of RrpA and Cys8 of RrpB, although the exact species which effects this
889 oxidation is not known. It is also possible that Q/F- Cys adduct formation (by Michael
890 addition) may occur (dashed line). Oxidized/modified RrpA C13 to C13-SO₂H leads to an
891 increased activation of the divergently transcribed gene *mdaB*, leading to production of
892 MdaB, which is a quinone reductase that can fully reduce quinones to quinols (HQ) by two-
893 electron transfer from NADPH. RrpB is a negative regulator of the divergently transcribed
894 *nfrA* gene, encoding an NADPH dependent flavin reductase (NfrA). We presume that
895 oxidation/modification of RrpB C8-SH produces a C8-SO₂-SH and C8-Dha (dehydroalanine)
896 which destabilizes the dimer and in turn leads to the de-repression of *nfrA* expression,
897 allowing NfrA to catalyze the formation of fully reduced flavin hydroquinone (FHQ). The
898 two-electron transfer catalyzed by both MdaB and NfrA avoids the semiquinone-mediated
899 production of ROS. It is not known if or how cycling back to the oxidized forms occurs. This
900 mechanism leads to a decrease in the toxic threat from exogenous quinones and flavins, but it
901 comes at the expense of a drain on the cellular NADPH pool.

902 **Table 1. Significantly differentially expressed genes at mid-log growth phase in the mutant strains $\Delta rrpA$, $\Delta rrpB$ and $\Delta rrpAB$**

Strain	Gene name	Product	Function	Log ² Fold
11168H $\Delta rrpA$	<i>cj1677 (capA)</i>	CapA – Campylobacter adhesion protein	Adhesion protein	2.17
	<i>cj1545c (mdaB)</i>	MdaB -NAD(P)H-quinone reductase	Putative reductase	-1.98*
	<hr/>			
11168H $\Delta rrpB$	<i>cj1556 (rrpB)</i>	RrpB - MarR-like transcriptional regulator	Putative transcriptional regulator	3.85
	<i>cj1555c (nfrA)</i>	NfrA - Putative NAD(P)-dependent reductase	Putative reductase	2.81
	<i>cj1677 (capA)</i>	CapA	Campylobacter adhesion protein A	1.88
	<hr/>			
11168H $\Delta rrpAB$	<i>cj1556 (rrpB)</i>	RrpB	Putative transcriptional regulator	3.17
	<i>cj1555c (nfrA)</i>	NfrA - Putative NAD(P)-dependent reductase	Putative reductase	2.50
	<i>cj1719c (leuA)</i>	LeuA - 2-isopropylmalate synthase	Amino acid biosynthesis	1.98
	<i>cj1546 (rrpA)</i>	RrpA - MarR-like transcriptional regulator	Putative transcriptional regulator	1.77
	<hr/>			
	<i>cj1454c (rimO)</i>	RimO - methylthiotransferase	Ribosomal protein methylthiotransferase	1.69
	<i>cj1710c (rmJ)</i>	Rnj - Ribonuclease J	An RNase that has 5'-3' exonuclease and possibly endonuclease activity	1.69
	<i>cj1711c (ksgA)</i>	KsgA/RsmA - methyltransferase	Ribosomal RNA small subunit methyltransferase A	1.60
	<i>cj0724</i>	Putative Molybdenum cofactor biosynthesis protein	Uncharacterized	-2.01
	<i>cj0265c (torB)</i>	Cytochrome C-type heme-binding periplasmic protein	Putative cytochrome C-type heme- binding periplasmic protein	-1.50

903 * Individual statistical test indicated gene was upregulated ($p < 0.05$).904 For the complete dataset for 11168H and $\Delta rrpA$, $\Delta rrpB$ and $\Delta rrpAB$ mutants see **Table. S1a**, **Table. S1b** and **Table. S1c**.

905 **Table 2.** PTM identification following database searching and manual verification of the matched fragmentation spectra for RrpA_{his6} and
 906 RrpB_{his6} proteins.
 907

Sample	Peptide	m/z	Charge	Mass	Residue	TIC intensity
RrpA (Control)	⁴ ENSPC _{Dha} NFEEC _{diox} GFNYTLALINGK ²⁵	821.03	3	2460.1	Cys8; Cys13	208300
	²⁸ MSILYC _{Dha} LFR ³⁶	556.30	2	1110.6	Cys33	204200
	²⁸ M _{ox} SILYC _{Dha} LFR ³⁶	564.30	2	1126.6	Met28; Cys33	110600
RrpA (2-hydroxy-1,4-naphthoquinone)	⁴ ENSPC _{Dha} NFEEC _{diox} GFNYTLALINGK ²⁵	821.03	3	2460.1	Cys8; Cys13	1119000
	²⁸ MSILYC _{Dha} LFR ³⁶	556.30	2	1110.6	Cys33	877900
RrpA (H₂O₂)	⁴ ENSPC _{Dha} NFEEC _{diox} GFNYTLALINGK ²⁵	821.03	3	2460.1	Cys8; Cys13	849400
	²⁸ M _{ox} SILYC _{Dha} LFR ³⁶	564.30	2	1126.6	Met28; Cys33	259400
RrpB (Control)	⁴ YHSLC _{sulfdiox} PIETTLNLIGNK ²⁰	990.48	2	1979	Cys8	37140
RrpB (H₂O₂)	⁴ YHSLC _{sulfdiox} PIETTLNLIGNK ²⁰	990.48	2	1979	Cys8	82780

908

909

910 Complete data set is presented in **Table. S2.**

